
SHORTCUTS AND IDENTIFIABILITY IN CONCEPT-BASED MODELS FROM A NEURO-SYMBOLIC LENS

A PREPRINT

Samuele Bortolotti*
DISI, University of Trento, Italy
name.surname@unitn.it

Emanuele Marconato*
DISI, University of Trento, Italy
DI, University of Pisa, Italy
name.surname@unitn.it

Paolo Morettin
DISI, University of Trento, Italy
name.surname@unitn.it

Andrea Passerini
DISI, University of Trento, Italy
name.surname@unitn.it

Stefano Teso
CIMeC & DISI, University of Trento, Italy
name.surname@unitn.it

February 18, 2025

ABSTRACT

Concept-based Models are neural networks that learn a concept extractor to map inputs to high-level *concepts* and an *inference layer* to translate these into predictions. Ensuring these modules produce interpretable concepts and behave reliably in out-of-distribution is crucial, yet the conditions for achieving this remain unclear. We study this problem by establishing a novel connection between Concept-based Models and *reasoning shortcuts* (RSs), a common issue where models achieve high accuracy by learning low-quality concepts, even when the inference layer is *fixed* and provided upfront. Specifically, we first extend RSs to the more complex setting of Concept-based Models and then derive theoretical conditions for identifying both the concepts and the inference layer. Our empirical results highlight the impact of reasoning shortcuts and show that existing methods, even when combined with multiple natural mitigation strategies, often fail to meet these conditions in practice.

1 Introduction

Concept-based Models (CBMs) are a broad class of self-explainable classifiers [Alvarez-Melis and Jaakkola, 2018, Koh et al., 2020, Espinosa Zarlenga et al., 2022, Marconato et al., 2022, Taeb et al., 2022] designed for high performance and *ante-hoc* interpretability. Learning a CBM involves solving two conjoint problems: acquiring high-level *concepts* describing the input (e.g., an image) and an *inference layer* that predicts a label from them. In many applications, it is essential that these two elements are “high quality”, in the sense that: *i*) the concepts should be *interpretable*, as failure in doing so compromises understanding [Schwalbe, 2022, Poeta et al., 2023] and steerability [Teso et al., 2023, Gupta and Narayanan, 2024], both key selling point of CBMs; and *ii*) the concepts and inference layer should behave well also *out of distribution* (OOD), e.g., they should not pick up spurious correlations between the input, the concepts and the output [Geirhos et al., 2020, Bahadori and Heckerman, 2021, Stammer et al., 2021].

It is natural to ask under what conditions CBMs can acquire such “high-quality” concepts and inference layers. While existing studies focus on concept quality [Mahinpei et al., 2021, Zarlenga et al., 2023, Marconato et al., 2023a], they neglect the role of the inference layer altogether. In contrast, we cast the question in terms of whether it is possible to *identify* from data concepts and inference layers with the intended semantics, defined formally in Section 3.1. We proceed to answer this question by building a novel connection with *reasoning shortcuts* (RSs), a well-known issue in Neuro-Symbolic (NeSy) AI whereby models achieve high accuracy

* Equal contribution. Correspondence to name.surname@unitn.it.

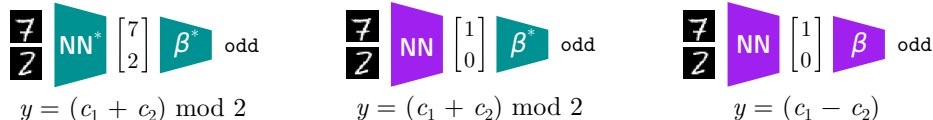


Figure 1: **Joint reasoning shortcuts.** The goal is to predict whether the sum of two MNIST digits is odd (as in Example 1) from a training set of all possible unique (even, even), (odd, odd), and (odd, even) pairs of MNIST digits. **Green** elements are fixed, **purple** ones are learned. **Left:** ground-truth concepts and inference layer. **Middle:** NeSy-CBMs with given knowledge can learn reasoning shortcuts, i.e., concepts with unintended semantics. **Right:** CBMs can learn joint reasoning shortcuts, i.e., both concepts and inference layer have unintended semantics.

by learning low-quality concepts *even if the inference layer is fixed* [Chang et al., 2020, Marconato et al., 2023b, Wang et al., 2023, Yang et al., 2024a]. E.g., a NeSy model for autonomous driving whose inference layer encodes the traffic laws might confuse pedestrians with red lights, as both entail the same prediction (the car has to stop) [Bortolotti et al., 2024].

We generalize RSs to CBMs in which *the inference layer is learned*, and supervision on the concepts may be absent. Our analysis shows that shortcut solutions can be exponentially many (indeed, we count them explicitly in Appendix B.2) and that, in general, maximum likelihood training is insufficient for attaining intended semantics. This negatively affects interpretability – as the learned concepts cannot be easily mapped to the ground-truth annotations – and OOD behavior. On the positive side, we also specify conditions under which (under suitable assumptions) CBMs *cannot* be fooled by RSs, proving that *the ground-truth concepts and inference layer can be identified* (see Theorem 3.8).

Our numerical simulations with regular and NeSy CBMs on several learning tasks suggest CBMs can be severely impacted by reasoning shortcuts in practice, as expected, and also that unfortunately the benefits of popular mitigation strategies do not carry over to this more challenging problem. These results cast doubts on the ability of these models to identify concepts and inference layers with the intended semantics unless appropriately nudged.

Contributions: In summary, we:

- Generalize reasoning shortcuts to the challenging case of CBMs whose inference layer is learned.
- Study conditions for maximum likelihood training to *identify* high quality concepts *and* inference layers.
- Present empirical evidence that proven mitigations fail in this challenging problem.

2 Preliminaries

Concept-based Models (CBMs) first map the input $\mathbf{x} \in \mathbb{R}^n$ into k discrete concepts $\mathbf{c} = (c_1, \dots, c_k) \in \mathcal{C}$ via a neural backbone, and then infer labels $\mathbf{y} \in \mathcal{Y}$ from this using a white-box layer, e.g., a linear layer. This setup makes it easy to figure out what concepts are most responsible for any prediction, yielding a form of *ante-hoc* concept-based interpretability. Several architectures follow this recipe, including approaches for converting black-box neural network classifiers into CBMs [Yuksekgonul et al., 2022, Wang et al., 2024, Dominici et al., 2024, Marcinkevičs et al., 2024].

A key issue is how to ensure the concepts are interpretable. Some CBMs rely on *concept annotations* [Koh et al., 2020, Sawada and Nakamura, 2022, Espinosa Zarlenga et al., 2022, Marconato et al., 2022, Kim et al., 2023, Debot et al., 2024]. These are however expensive to obtain, prompting researchers to replace them with (potentially unreliable [Huang et al., 2024, Sun et al., 2024]) annotations obtained from foundation models [Oikarinen et al., 2022, Yang et al., 2023, Srivastava et al., 2024] or *unsupervised* concept discovery [Alvarez-Melis and Jaakkola, 2018, Chen et al., 2019, Taeb et al., 2022, Schrodi et al., 2024].

Neuro-Symbolic CBMs (NeSy-CBMs) specialize CBMs to tasks in which the prediction $\mathbf{y} \in \mathcal{Y}$ ought to comply with known safety or structural constraints. These are supplied as a formal specification – a logic formula K , *aka knowledge* – tying together the prediction \mathbf{y} and the concepts \mathbf{c} . In NeSy-CBMs, the inference step is a *symbolic reasoning layer* that steers [Lippi and Frasconi, 2009, Diligenti et al., 2012, Donadello et al., 2017, Xu et al., 2018] or guarantees [Manhaeve et al., 2018, Giunchiglia and Lukasiewicz, 2020, Hoernle et al., 2022, Ahmed et al., 2022] the labels and concepts to be logically consistent according to K . Throughout, we will consider the following example task:

Example 1 (MNIST-SumParity). Given two MNIST digits [LeCun, 1998], we wish to predict whether their sum is even or odd. The numerical values of the two digits can be modelled as concepts $\mathbf{C} \in \{0, \dots, 9\}^2$, and the inference layer is entirely determined by the prior knowledge: $\mathbf{K} = ((y = 1) \Leftrightarrow (C_1 + C_2) \text{ is odd})$. This specifies that the label $y \in \{0, 1\}$ ought to be consistent with the predicted concepts \mathbf{C} . See Fig. 1 for an illustration.

Like CBMs, NeSy-CBMs are usually trained via *maximum likelihood* and gradient descent, but without concept supervision. The reasoning layer is typically imbued with fuzzy [Zadeh, 1988] or probabilistic [De Raedt and Kimmig, 2015] logic semantics to ensure differentiability. Many NeSy-CBMs require \mathbf{K} to be provided upfront, as in Example 1, hence their inference layer has no learnable parameters. Starting with Section 3, we will instead consider NeSy-CBMs that – just like regular CBMs – *learn the inference layer* [Wang et al., 2019, Liu et al., 2023, Daniele et al., 2023, Tang and Ellis, 2023, Wüst et al., 2024].

2.1 Reasoning Shortcuts

Before discussing reasoning shortcuts, we need to establish a clear relationship between concepts, inputs, and labels. The RS literature does so by assuming the following *data generation process* [Marconato et al., 2023b, Yang et al., 2024a, Umili et al., 2024]: each input $\mathbf{x} \in \mathbb{R}^n$ is the result of sampling k *ground-truth concepts* $\mathbf{g} = (g_1, \dots, g_k) \in \mathcal{G}$ (e.g., in MNIST-SumParity two numerical digits) from an unobserved distribution $p^*(\mathbf{G})$ and then \mathbf{x} itself (e.g., two corresponding MNIST images) from the conditional distribution $p^*(\mathbf{X} | \mathbf{g})$.² Labels $\mathbf{y} \in \mathcal{Y}$ are sampled from the conditional distribution of \mathbf{g} given by $p^*(\mathbf{Y} | \mathbf{g}; \mathbf{K})$ consistently with \mathbf{K} (e.g., $y = 1$ if and only if $g_1 + g_2$ is odd). The ground-truth distribution is thus:

$$p^*(\mathbf{X}, \mathbf{Y}) = \mathbb{E}_{\mathbf{g} \sim p^*(\mathbf{G})} [p^*(\mathbf{X} | \mathbf{g}) p^*(\mathbf{Y} | \mathbf{g}; \mathbf{K})] \quad (1)$$

Intuitively, a *reasoning shortcut* (RS) occurs when a NeSy-CBM with *fixed* knowledge \mathbf{K} attains high or even perfect label accuracy by learning concepts \mathbf{C} that differ from the ground-truth ones \mathbf{G} [Marconato et al., 2023b]. As commonly done, we work in the setting where $\mathcal{G} = \mathcal{C}$.

Example 2. In MNIST-SumParity, a NeSy model can achieve perfect accuracy by mapping each pair of MNIST images $\mathbf{x} = (\mathbf{x}_1, \mathbf{x}_2)$ to the corresponding ground-truth digits, that is, $\mathbf{c} = (g_1, g_2)$. However, it would achieve the same accuracy if it were to map it to $\mathbf{c} = (g_1 \bmod 2, g_2 \bmod 2)$, as doing so leaves the parity of the sum unchanged, see Fig. 1. Hence, a NeSy model cannot distinguish between the two based on label likelihood alone during training.

RSs by definition yield good labels in-distribution, yet they compromise out-of-distribution (OOD) performance. For instance, in autonomous driving tasks, NeSy-CBMs can confuse the concepts of “pedestrian” and “red light”, leading to poor decisions for OOD decisions where the distinction matters [Bortolotti et al., 2024]. The meaning of concepts affected by RSs is unclear, affecting understanding [Schwalbe, 2022], intervenability [Shin et al., 2023, Espinosa Zarlenga et al., 2024, Steinmann et al., 2024b], debugging [Lertvittayakumjorn et al., 2020, Stammer et al., 2021] and down-stream applications that hinge on concepts being high-quality, like NeSy formal verification [Xie et al., 2022, Zaid et al., 2023, Morettin et al., 2024]. Unfortunately, existing works on RSs do not apply to CBMs and NeSy-CBMs where the inference layer is learned.

3 Reasoning Shortcuts in CBMs

Given a finite set \mathcal{S} , we indicate with $\Delta_{\mathcal{S}} \subset [0, 1]^{|\mathcal{S}|}$ the simplex of probability distributions $P(\mathcal{S})$ over items in \mathcal{S} . Notice that the set of its vertices $\text{Vert}(\Delta_{\mathcal{S}})$ contains all point mass distributions $\mathbb{1}\{S = s\}$ for all $s \in \mathcal{S}$.

CBMs as pairs of functions. CBMs and NeSy-CBMs differ in how they implement the inference layer, hence to bridge them we employ the following unified formalism. Any CBM can be viewed as a pair of learnable functions implementing the concept extractor and the inference layer, respectively, cf. Fig. 2. Formally, the former is a function $\mathbf{f} : \mathbb{R}^n \rightarrow \Delta_{\mathcal{C}}$ mapping inputs \mathbf{x} to a conditional distribution $p(\mathbf{C} | \mathbf{x})$ over the concepts, however it can be better understood as a function $\alpha : \mathcal{G} \rightarrow \Delta_{\mathcal{C}}$ taking ground-truth concepts \mathbf{g} as input instead, and defined as:

$$\alpha(\mathbf{g}) = \mathbb{E}_{\mathbf{x} \sim p^*(\mathbf{X} | \mathbf{g})} [\mathbf{f}(\mathbf{x})] \quad (2)$$

On the other hand, the inference layer is a function $\omega : \Delta_{\mathcal{C}} \rightarrow \Delta_{\mathcal{Y}}$ mapping the concept distribution output by the concept extractor into a label distribution $p(\mathbf{Y} | \mathbf{f}(\mathbf{x}))$. For clarity, we also define $\beta : \mathcal{C} \rightarrow \Delta_{\mathcal{Y}}$, which is

²This distribution subsumes stylistic factors, e.g., calligraphy.

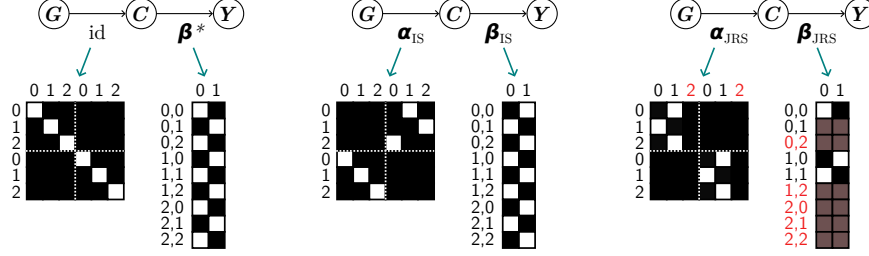


Figure 2: **Examples of semantics in MNIST-SumParity** restricted to $g, c \in \{0, 1, 2\}^2$ for readability. **Left:** ideally, α should be the identity (i.e., C recovers the ground-truth concepts G) and the inference layer should learn β^* . **Middle:** $(\alpha_{IS}, \beta_{IS}) \neq (\text{id}, \beta^*)$ has intended semantics (Definition 3.3), i.e., the ground-truth concepts and inference layer can be easily recovered and generalize OOD. **Right:** $(\alpha_{JRS}, \beta_{JRS})$ affected by the JRS in Fig. 1. Elements (predicted concepts C and entries in β) in red are never predicted nor used, highlighting *simplicity bias*. Maps are visualized as matrices.

identical to the former except it works with concept *values* rather than *distributions*, that is:

$$\beta(\mathbf{c}) := \omega(\mathbb{1}\{C = \mathbf{c}\}) \quad (3)$$

Hence, a CBM entails both a pair $(\mathbf{f}, \omega) \in \mathcal{F} \times \Omega$ and a pair $(\alpha, \beta) \in \mathcal{A} \times \mathcal{B}$.³ Later on, we will make use of the fact that \mathcal{A} and \mathcal{B} are *simplices* [Morton, 2013, Montúfar et al., 2014], i.e., each $\alpha \in \mathcal{A}$ (resp. $\beta \in \mathcal{B}$) can be written as a convex combination of vertices $\text{Vert}(\mathcal{A})$ (resp. $\text{Vert}(\mathcal{B})$).

As mentioned in Section 2, supplying prior knowledge K to a NeSy-CBM is equivalent to *fixing the inference layer* to a corresponding function ω^* (and β^*). Note that whereas ω^* changes based on how reasoning is implemented – e.g., fuzzy vs. probabilistic logic – β^* does not, as both kinds of reasoning layers behave identically when input any point-mass concept distribution $\mathbb{1}\{C = \mathbf{c}\}$.

Standard assumptions. The maps α and β are especially useful for analysis provided the following two standard assumptions about how data are distributed:

Assumption 3.1 (Invertibility). *The ground-truth distribution $p^*(G | X)$ is induced by a function $\mathbf{f}^* : \mathbf{x} \mapsto \mathbf{g}$, i.e., $p^*(G | X) = \mathbb{1}\{G = \mathbf{f}^*(X)\}$.*

This means that the ground-truth concepts \mathbf{g} can always be unambiguously recovered for all inputs \mathbf{x} by a sufficiently expressive concept extractor; the α it induces is the identity, indicated as $\text{id}(\mathbf{g}) := \mathbb{1}\{C = \mathbf{g}\} \in \text{Vert}(\mathcal{A})$.

Assumption 3.2 (Deterministic knowledge). *The ground-truth distribution $p^*(Y | G; K)$ is induced by the knowledge via a map $\beta^* \in \text{Vert}(\mathcal{B})$, such that $p^*(Y | G; K) = \beta^*(\mathbf{g})$.*

This ensures that the labels \mathbf{y} can be predicted without any ambiguity from the ground-truth concepts \mathbf{g} . Both assumptions apply in several tasks, see [Bortolotti et al., 2024]. The maximum log-likelihood objective is then written as:

$$\max_{(\mathbf{f}, \omega) \in \mathcal{F} \times \Omega} \mathbb{E}_{(\mathbf{x}, \mathbf{y}) \sim p^*(\mathbf{X}, \mathbf{Y})} \log(\omega_{\mathbf{y}} \circ \mathbf{f})(\mathbf{x}) \quad (4)$$

Here, $\omega_{\mathbf{y}}$ is the conditional probability of the ground-truth labels \mathbf{y} . Notice that under the above assumptions CBMs attaining maximum likelihood perfectly model the ground-truth data distribution $p^*(\mathbf{X}, \mathbf{Y})$, see Lemma C.1.

3.1 Intended Semantics and Joint Reasoning Shortcuts

We posit that a CBM $(\alpha, \beta) \in \mathcal{A} \times \mathcal{B}$ has “high-quality” concepts and inference layer if it satisfies two desiderata:

- **Disentanglement:** each learned concept C_i should be equal to a single ground-truth concept G_j up to an invertible transformation;
- **Generalization:** the combination of α and β must always yield correct predictions.

³We work in the non-parametric setting, hence \mathcal{F} and Ω contain all learnable concept extractors \mathbf{f} and inference layers ω , and similarly \mathcal{A} and \mathcal{B} contain all learnable maps α and β .

In our setting, without concept supervision and prior knowledge, the learned concepts are *anonymous* and users have to figure out which is which in a *post-hoc* fashion, e.g., by aligning them to dense annotations [Koh et al., 2020, Espinosa Zarlenga et al., 2022, Daniele et al., 2023, Tang and Ellis, 2023]. Doing so is also a prerequisite for understanding the learned inference layer [Wüst et al., 2024, Daniele et al., 2023, Espinosa Zarlenga et al., 2022, 2024]. The benefit of *disentanglement* is that when it holds the mapping between \mathbf{G} and \mathbf{C} can be recovered *exactly* using Hungarian matching [Kuhn, 1955]; otherwise it is arbitrarily difficult to recover, hindering interpretability. This links CBMs with many works that treat model representations’ *identifiability* in Independent Component Analysis and Causal Representation Learning [Khemakhem et al., 2020b, Gresele et al., 2021, Lippe et al., 2023, Lachapelle et al., 2023, von Kügelgen et al., 2024], where disentanglement plays a central role. *Generalization* is equally important, as it entails that CBMs generalize beyond the support of training data and yields sensible OOD behavior, i.e., output the same predictions that would be obtained by using the ground-truth pair. Since we want α to be disentangled, this implies, in turn, a specific form for the map β , as shown by the next definition, which formalizes these desiderata:

Definition 3.3 (Intended Semantics). *A CBM $(\mathbf{f}, \omega) \in \mathcal{F} \times \Omega$ entailing a pair $(\alpha, \beta) \in \mathcal{A} \times \mathcal{B}$ possesses the intended semantics if there exists a permutation $\pi : [k] \rightarrow [k]$ and k element-wise invertible functions ψ_1, \dots, ψ_k such that:*

$$\alpha(\mathbf{g}) = (\psi \circ \mathbf{P}_\pi \circ \text{id})(\mathbf{g}) \quad (5)$$

$$\beta(\mathbf{c}) = (\beta^* \circ \mathbf{P}_\pi^{-1} \circ \psi^{-1})(\mathbf{c}) \quad (6)$$

Here, $\mathbf{P}_\pi : \mathcal{C} \rightarrow \mathcal{C}$ is the permutation matrix induced by π and $\psi(\mathbf{c}) := (\psi_1(c_1), \dots, \psi_k(c_k))$. In this case, we say that (α, β) is equivalent to (id, β^*) , i.e., $(\alpha, \beta) \sim (\text{id}, \beta^*)$.

That is, intended semantics holds if the learned concepts \mathbf{C} match the ground-truth concepts \mathbf{G} modulo simple invertible transformations – like reordering and negation (Eq. (5)) – and the inference layer *undoes* these transformations before applying the “right” inference layer β^* (Eq. (6)). This also means that CBMs satisfying them are *equivalent* – in a very precise sense – to the ground-truth pair (id, β^*) . A similar equivalence relation was analyzed for continuous representations in energy-based models, including supervised classifiers, by Khemakhem et al. [2020b]. In Lemma C.4, we prove that models with the intended semantics yield the same predictions of the ground-truth pair for all $\mathbf{g} \in \mathcal{G}$.

Training a (NeSy) CBM via maximum likelihood does not guarantee it will embody intended semantics. We denote these failure cases as *joint reasoning shortcuts* (JRSs):

Definition 3.4 (Joint Reasoning Shortcut). *Take a CBM $(\mathbf{f}, \omega) \in \mathcal{F} \times \Omega$ that attains optimal log-likelihood (Eq. (4)). The pair (α, β) entailed by it (Eqs. (2) and (3)) is a JRSs if it does not possess the intended semantics (Definition 3.3), i.e., $(\alpha, \beta) \not\sim (\text{id}, \beta^*)$.*

JRSs can take different forms. First, even if the learned inference layer β matches (modulo \mathbf{P}_π and ψ) the ground-truth one β^* , α might not match (also modulo \mathbf{P}_π and ψ) the identity. This is analogous to regular RSs in NeSy CBMs (Section 2), in that the learned concepts do not reflect the ground-truth ones: while this is sufficient for high in-distribution performance (the training likelihood is in fact optimal), it may yield poor OOD behavior. Second, even if α matches the identity, the inference layer β might not match the ground-truth one β^* . In our experiments Section 5, we observe that this often stems from *simplicity bias* [Yang et al., 2024b], i.e., the CBM’s inference layer tends to acquire specialized functions β that are much simpler than β^* , leading to erroneous predictions OOD. Finally, neither the inference layer β nor the map α might match the ground-truth, opening the door to additional failure modes. Consider the following example:

Example 3. *Consider a MNIST-SumParity problem where the training set consists of all possible unique (even, even), (odd, odd), and (odd, even) pairs of MNIST digits, as in Fig. 1. A CBM trained on this data would achieve perfect accuracy by learning a JRS that extracts the parity of each input digit, yielding two binary concepts in $\{0, 1\}$, and computes the difference between these two concepts. This JRS involves **much simpler concepts and knowledge** compared to the ground-truth ones. It also mispredicts all OOD pairs where the even digits come before odd digits.*

3.2 Theoretical Analysis

We proceed to determine how many *deterministic* JRSs $(\alpha, \beta) \in \text{Vert}(\mathcal{A}) \times \text{Vert}(\mathcal{B})$ a learning task admits, and then show in Theorem 3.8 that this number determines the presence or absence of general (non-deterministic) JRSs.

Theorem 3.5 (Informal). *Under Assumptions 3.1 and 3.2, the number of deterministic JRSs (α, β) is:*

$$\sum_{(\alpha, \beta)} \mathbb{1}\left\{ \bigwedge_{\mathbf{g} \in \text{supp}(\mathbf{G})} (\beta \circ \alpha)(\mathbf{g}) = \beta^*(\mathbf{g}) \right\} - C[\mathcal{G}] \quad (7)$$

where the sum runs over $\text{Vert}(\mathcal{A}) \times \text{Vert}(\mathcal{B})$, and $C[\mathcal{G}]$ is the total number of pairs with the intended semantics.

All proofs can be found in [Appendix C](#). Intuitively, the first count runs over all deterministic pairs (α, β) that achieve maximum likelihood on the training set (i.e., the predicted labels $(\beta \circ \alpha)(\mathbf{g})$ matches the ground-truth labels $\beta^*(\mathbf{g})$ for all ground-truth concepts \mathbf{g} appearing in the data), while the second term subtracts the pairs (α, β) that possess the intended semantics as per [Definition 3.3](#). Whenever the count is larger than zero, a CBM trained via maximum likelihood *can* learn a deterministic JRS.

As a sanity check, we show that if prior knowledge \mathbf{K} is provided – fixing the inference layer to β^* – the number of deterministic JRSs in fact matches that of RSs, as expected:

Corollary 3.6. *Consider a fixed $\beta^* \in \text{Vert}(\mathcal{B})$. Under Assumptions 3.1 and 3.2, the number of deterministic JRSs $(\alpha, \beta^*) \in \text{Vert}(\mathcal{A}) \times \text{Vert}(\mathcal{B})$ is:*

$$\sum_{\alpha \in \text{Vert}(\mathcal{A})} \mathbb{1}\left\{ \bigwedge_{\mathbf{g} \in \text{supp}(\mathbf{G})} (\beta^* \circ \alpha)(\mathbf{g}) = \beta^*(\mathbf{g}) \right\} - 1 \quad (8)$$

This matches the count for deterministic RSs in [\[Marconato et al., 2023b\]](#).

A natural consequence of [Corollary 3.6](#) that whenever $|\text{Vert}(\mathcal{B})| > 1$ the number of deterministic JRSs in [Eq. \(7\)](#) can be substantially **larger** than the number of deterministic RSs [Eq. \(8\)](#). For instance, in MNIST-SumParity with digits restricted to the range $[0, 4]$ there exist exactly 64 RSs but about 100 *thousand* JRSs, and the gap increases as we extend the range $[0, N]$. We provide an in-depth analysis in [Appendix B.2](#).

Next, we show that whenever the number of deterministic JRSs in [Eq. \(7\)](#) is zero, there exist **no JRSs at all**, including non-deterministic ones. This however only applies to CBMs that satisfy the following natural assumption:

Assumption 3.7 (Extremality). *The inference layer $\omega \in \Omega$ satisfies extremality if, for all $\lambda \in (0, 1)$ and for all $\mathbf{c} \neq \mathbf{c}' \in \mathcal{C}$ such that $\arg\max_{\mathbf{y} \in \mathcal{Y}} \omega(\mathbb{1}\{\mathbf{C} = \mathbf{c}\})_{\mathbf{y}} \neq \arg\max_{\mathbf{y} \in \mathcal{Y}} \omega(\mathbb{1}\{\mathbf{C} = \mathbf{c}'\})_{\mathbf{y}}$, it holds:*

$$\begin{aligned} & \max_{\mathbf{y} \in \mathcal{Y}} \omega(\lambda \mathbb{1}\{\mathbf{C} = \mathbf{c}\} + (1 - \lambda) \mathbb{1}\{\mathbf{C} = \mathbf{c}'\})_{\mathbf{y}} \\ & \leq \max \left(\max_{\mathbf{y} \in \mathcal{Y}} \omega(\mathbb{1}\{\mathbf{C} = \mathbf{c}\})_{\mathbf{y}}, \max_{\mathbf{y} \in \mathcal{Y}} \omega(\mathbb{1}\{\mathbf{C} = \mathbf{c}'\})_{\mathbf{y}} \right) \end{aligned}$$

Intuitively, a CBM satisfies this assumption if its inference layer ω is “peaked”: for any two concept vectors \mathbf{c} and \mathbf{c}' yielding distinct predictions, the label probability output by ω for any mixture distribution thereof is no larger than the label probability that it associates to \mathbf{c} and \mathbf{c}' . That is, distributing probability mass across concepts never nets an advantage in terms of label likelihood. While this assumption does not hold for general CBMs, we show in [Appendix E](#) that it holds for popular architectures, including most of those that we experiment with. Under [Assumption 3.7](#), the next result holds:

Theorem 3.8 (Identifiability). *Under Assumptions 3.1 and 3.2, if the number of deterministic JRSs ([Eq. \(7\)](#)) is zero then every CBM $(\mathbf{f}, \omega) \in \mathcal{F} \times \Omega$ satisfying [Assumption 3.7](#) that attains maximum log-likelihood ([Eq. \(4\)](#)) possesses the intended semantics ([Definition 3.3](#)). That is, the pair $(\alpha, \beta) \in \mathcal{A} \times \mathcal{B}$ entailed by each such CBM is equivalent to the ground-truth pair (id, β^*) , i.e., $(\alpha, \beta) \sim (\text{id}, \beta^*)$.*

4 Practical Solutions

By [Theorem 3.8](#), getting rid of *deterministic* JRSs from a task prevents CBMs trained via maximum log-likelihood to learn JRS altogether. Next, we discuss strategies for achieving this goal and will assess them empirically in [Section 5](#). An in-depth technical analysis is left to [Appendix D](#).

4.1 Supervised strategies

The most direct strategies for controlling the semantics of learned CBMs rely on supervision. **Concept supervision** is the go-to solution for improving concept quality in CBMs [\[Koh et al., 2020, Chen et al., 2020b, Espinosa Zarlenga et al., 2022, Marconato et al., 2022\]](#) and NeSy-CBMs [\[Bortolotti et al., 2024, Yang et al.,](#)

2024a]. Supplying full concept supervision for all ground-truth concepts \mathbf{G} provably prevents learning α 's that do not match the identity. However, this does not translate into guarantees on the inference layer β , at least in tasks affected by confounding factors such as spurious correlations among concepts [Stammer et al., 2021]. E.g., if the i -th and j -th ground-truth concepts are strongly correlated, the inference layer β can interchangeably use either, regardless of what β^* does.

Another option is employing *knowledge distillation* [Hinton, 2015], that is, supplying supervision of the form (\mathbf{g}, \mathbf{y}) to encourage the learned knowledge β to be close to β^* for the supervised \mathbf{g} 's. This supervision is available for free provided concept supervision is available, but can also be obtained separately, e.g., by interactively collecting user interventions [Shin et al., 2023, Espinosa Zarlenga et al., 2024, Steinmann et al., 2024b]. This strategy cannot avoid *all* JRSs because even if $\beta = \beta^*$, the CBM may suffer from regular RSs (i.e., α does not match id).

Another option is to fit a CBM on *multiple tasks* [Caruana, 1997] sharing concepts. It is known that a NeSy-CBM attaining optimal likelihood on multiple NeSy tasks with different prior knowledges is also optimal for the *single* NeSy task obtained by conjoining those knowledges [Marconato et al., 2023b]: this more constrained knowledge better steers the semantics of the learned concepts, ruling out potential JRSs. Naturally, collecting a sufficiently large number of diverse tasks using the same concepts can be highly non-trivial, depending on the application.

4.2 Unsupervised strategies

Many popular strategies for improving concept quality in (NeSy) CBMs are unsupervised. A cheap but effective one when dealing with multiple inputs is to *process inputs individually*, preventing mixing between their concepts. E.g., In MNIST-SumParity one can apply the same digit extractor to each digit separately, while for images with multiple objects one can first segment them (e.g., with YoloV11 [Jocher et al., 2023]) and then process the resulting bounding boxes individually. This is extremely helpful for reducing, and possibly overcoming, RSs [Marconato et al., 2023b] and frequently used in practice [Manhaeve et al., 2018, van Krieken et al., 2022, Daniele et al., 2023, Tang and Ellis, 2023]. We apply it in all our experiments.

Both supervised [Marconato et al., 2022] and unsupervised [Alvarez-Melis and Jaakkola, 2018, Li et al., 2018] CBMs may employ a *reconstruction* penalty [Baldi, 2012, Kingma, 2013] to encourage learning informative concepts. Reconstruction can help prevent collapsing distinct ground-truth concepts into single learned concepts, e.g., in MNIST-SumParity the odd digits cannot be collapsed together without impairing reconstruction.⁴ Alternatively, one can employ *entropy maximization* [Manhaeve et al., 2021] to spread concept activations evenly across the bottleneck. This can be viewed as a less targeted but more efficient alternative to reconstruction, which becomes impractical for higher dimensional inputs. Another popular option is *contrastive learning* [Chen et al., 2020a], in that augmentations render learned concepts more robust to style variations [Von Kügelgen et al., 2021], e.g., for MNIST-based tasks it helps to cluster distinct digits in representation space [Sansone and Manhaeve, 2023]. Unsupervised strategies all implicitly counteract *simplicity bias* whereby α ends up collapsing.

5 Case Studies

We tackle the following key research questions:

- Q1. Are CBMs affected by JRSs in practice?
- Q2. Do JRSs affect interpretability and OOD behavior?
- Q3. Can existing mitigation strategies prevent JRSs?

Additional implementation details about the tasks, architectures, and model selection are reported in [Appendix A](#).

Models. We evaluate several (also NeSy) CBMs. DeepProbLog (DPL) [Manhaeve et al., 2018, 2021] is the *only* method supplied with the ground-truth knowledge \mathbf{K} , and uses probabilistic-logic reasoning to ensure predictions are consistent with it. CBNM is a Concept-Bottleneck Model [Koh et al., 2020] with no supervision on the concepts. Deep Symbolic Learning (DSL) [Daniele et al., 2023] is a SOTA NeSy-CBM that learns

⁴This is provably the case *context-style separation* i.e., assuming the concepts do not depend on the stylistic factor of the input like calligraphy [Marconato et al., 2023b, Proposition 6].

Table 1: Results for MNIST-Add.

| METHOD | $F_1(Y)$ (\uparrow) | $F_1(C)$ (\uparrow) | $Cls(C)$ (\downarrow) | $F_1(\beta)$ (\uparrow) |
|--------|-------------------------|-------------------------|---------------------------|-----------------------------|
| DPL | 0.98 ± 0.01 | 0.99 ± 0.01 | 0.01 ± 0.01 | – |
| CBNM | 0.98 ± 0.01 | 0.99 ± 0.01 | 0.01 ± 0.01 | 1.00 ± 0.01 |
| SENN | 0.97 ± 0.01 | 0.80 ± 0.07 | 0.01 ± 0.01 | 0.75 ± 0.08 |
| DSL | 0.96 ± 0.02 | 0.98 ± 0.01 | 0.01 ± 0.01 | 1.00 ± 0.01 |
| DPL* | 0.91 ± 0.09 | 0.92 ± 0.08 | 0.01 ± 0.01 | 0.90 ± 0.08 |
| bears* | 0.76 ± 0.15 | 0.87 ± 0.13 | 0.01 ± 0.01 | 0.67 ± 0.14 |

Table 2: Results for MNIST-SumParity.

| METHOD | $F_1(Y)$ (\uparrow) | $F_1(C)$ (\uparrow) | $Cls(C)$ (\downarrow) | $F_1(\beta)$ (\uparrow) |
|--------|-------------------------|-------------------------|---------------------------|-----------------------------|
| DPL | 0.99 ± 0.01 | 0.43 ± 0.08 | 0.36 ± 0.15 | – |
| CBNM | 0.90 ± 0.18 | 0.09 ± 0.03 | 0.66 ± 0.09 | 0.54 ± 0.04 |
| SENN | 0.99 ± 0.01 | 0.49 ± 0.05 | 0.01 ± 0.01 | 0.53 ± 0.06 |
| DSL | 0.94 ± 0.03 | 0.07 ± 0.01 | 0.80 ± 0.01 | 0.52 ± 0.01 |
| DPL* | 0.99 ± 0.01 | 0.07 ± 0.01 | 0.80 ± 0.01 | 0.50 ± 0.05 |
| bears* | 0.99 ± 0.01 | 0.30 ± 0.03 | 0.22 ± 0.04 | 0.36 ± 0.09 |

Table 3: Results for Clevr.

| METHOD | $F_1(Y)$ (\uparrow) | $F_1(C)$ (\uparrow) | $Cls(C)$ (\downarrow) | $F_1(\beta)$ (\uparrow) |
|--------|-------------------------|-------------------------|---------------------------|-----------------------------|
| DPL | 0.99 ± 0.01 | 0.25 ± 0.05 | 0.57 ± 0.02 | – |
| CBNM | 0.99 ± 0.01 | 0.19 ± 0.06 | 0.35 ± 0.09 | 0.01 ± 0.02 |
| DPL* | 0.99 ± 0.01 | 0.22 ± 0.04 | 0.57 ± 0.03 | 0.01 ± 0.01 |

concepts and symbolic knowledge jointly; it implements the latter as a truth table and reasoning using fuzzy logic. We also consider two variants: DPL* replaces fuzzy with probabilistic logic, while bears* wraps DPL* within BEARS [Marconato et al., 2024], an ensemble approach for handling regular RSs. In short, bears* consists of a learned inference layer and multiple concept extractors. The former is learned only once, the latter are learned sequentially. We also evaluate Self-explainable Neural Networks (SENN) [Alvarez-Melis and Jaakkola, 2018], unsupervised CBMs that include a reconstruction penalty. Since they do not satisfy our assumptions, they are useful to empirically assess the generality of our remarks.

Data sets. In order to assess both learned concepts and inference layer, we use three representative NeSy tasks with well-defined concept annotations and prior knowledge. MNIST-Add [Manhaeve et al., 2018] involves predicting the sum of two MNIST digits, and serves as a sanity check as it provably contains no RSs. MNIST-SumParity is similar except we have to predict the *parity* of the sum, as in Fig. 1, and admits many JRSs. We also include a variant of Clevr [Johnson et al., 2017] in which images belong to 3 classes as determined by a logic formula and only contain 2 to 4 objects, for scalability.

Metrics. For each CBM, we evaluate predicted labels and concepts with the F_1 score (resp. $F_1(Y)$ and $F_1(C)$) on the test split. Computing $F_1(C)$ requires to first align the predicted concepts to ground-truth annotations. We do so by using the Hungarian algorithm [Kuhn, 1955] to find a permutation π that maximizes the Pearson correlation across concepts. Concept collapse $Cls(C)$ quantifies to what extent the concept extractor blends different *ground-truth* concepts together: high collapse indicates that it predicts fewer concepts than expected. We measure the quality of the learned inference layer β as follows: for each example, we reorder the concept annotations g using π , feed the result to β and compute the F_1 score ($F_1(\beta)$) of its predictions. See Appendix A.4 for details.

Mitigation strategies. We evaluate all strategies discussed in Section 4 as well as a combination of all unsupervised mitigations, denoted H+R+C (entropy, reconstruction, contrastive). Implementations are taken verbatim from [Bortolotti et al., 2024]. For contrastive learning, we apply an InfoNCE loss to the predicted concept distribution with the augmentations suggested by Chen et al. [2020a]. For knowledge distillation, the inference layer is fed ground-truth concepts and trained to optimize the log-likelihood of the corresponding labels.

Q1: All tested CBMs suffer from JRSs and simplicity bias. We analyze three learning tasks of increasing complexity. MNIST-Add provably contains no JRSs and thus satisfies the preconditions of Theorem 3.8. Compatibly with this result, all CBMs attain high label performance ($F_1(Y) \geq 90\%$) and high-quality semantics, as shown by the values of $F_1(C)$ ($\geq 90\%$) and $F_1(\beta)$ ($\geq 75\%$) seen in Table 1. The only exception

Table 4: CBNM on biased MNIST-SumParity.

| C-SUP | K-SUP | ID | | OOD | |
|-------|-------|-------------------------|-----------------------------|-------------------------|-----------------------------|
| | | $F_1(Y)$ (\uparrow) | $F_1(\beta)$ (\uparrow) | $F_1(Y)$ (\uparrow) | $F_1(\beta)$ (\uparrow) |
| 0% | 0% | 0.99 ± 0.01 | 0.55 ± 0.05 | 0.01 ± 0.01 | 0.47 ± 0.07 |
| 0% | 100% | 0.99 ± 0.01 | 0.56 ± 0.06 | 0.01 ± 0.01 | 0.58 ± 0.08 |
| 100% | 0% | 0.97 ± 0.01 | 0.88 ± 0.04 | 0.40 ± 0.14 | 0.31 ± 0.12 |
| 100% | 100% | 0.97 ± 0.01 | 0.95 ± 0.01 | 0.97 ± 0.02 | 0.69 ± 0.27 |

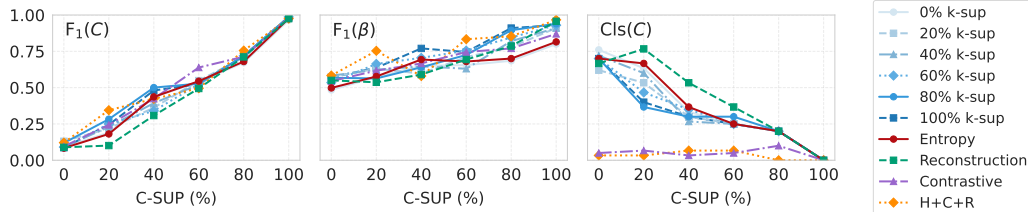


Figure 3: **Traditional mitigations have limited effect** on CBNM (top) and DPL* (bottom) for MNIST-SumParity. The only outlier is contrastive learning (orange and purple lines), which consistently ameliorates concept collapse.

is bears*, which by design trades off performance for calibration. However, in MNIST-SumParity and Clevr,⁵ which are more complex, *all models lack intended semantics*. This is clear from Tables 2 and 3: despite attaining high $F_1(Y)$ ($\geq 90\%$), the learned concepts and inference layer are both low quality: $F_1(C)$ is always low – it never crosses the 50% mark – and $F_1(\beta)$ is at best around chance level.

The behavior of concept collapse strongly hints at *simplicity bias*. While no collapse takes place in MNIST-Add ($\text{Cls}(C) \leq 0.01$, i.e., digits are not compacted together), in MNIST-SumParity and Clevr collapse is omnipresent ($\text{Cls}(C) \geq 0.22$), suggesting that CBMs are prone to simplicity bias, as expected. SENN is an outlier, likely due to the higher capacity of its inference layer (rather than reconstruction, which is entirely ineffective in Q3). Even having access to the ground-truth knowledge is ineffective, as show by the high degree of collapse displayed by DPL.

Q2: JRSs compromise OOD behavior and supervision only partially helps. We evaluate the impact of JRSs and supervision on OOD behavior by training a CBNM on the biased version of MNIST-SumParity in Fig. 1. The in-distribution (ID) data comprise all (odd, odd), (even, even), and (odd, even) pairs of MNIST digits, while the OOD split contains all (even, odd) pairs. Table 4 lists results on both ID and OOD test sets for varying percentages of concept and knowledge supervision. While all models produce high-quality predictions in-distribution ($F_1(Y) \geq 0.97$), only the CBNM receiving complete supervision attains acceptable OOD predictions: for the others, $F_1(Y) \leq 0.40$. Even in this case, though, the inference layer still does not have intended semantics, as shown by $F_1(\beta) \leq 70\%$.

Q3: Popular CBM and RS mitigations fall short. Finally, we apply each mitigation strategy to a CBNM trained on MNIST-SumParity and Clevr, ablating the amount of supervision. The results for MNIST-SumParity in Fig. 3 show while concept supervision (x -axis) helps all metrics, adding reconstruction, entropy maximization, and contrastive learning to the mix brings no benefits for concept ($F_1(C)$) and knowledge ($F_1(\beta)$) quality, not even when combined (orange curve). Knowledge supervision is similarly ineffective (blue lines). This is not unexpected: MNIST-SumParity and Clevr suffer from RSs even when the model is supplied the prior knowledge. The only noticeable improvement comes from contrastive learning for concept collapse ($\text{Cls}(C)$): the orange and purple curves in Fig. 3 (right) show it can effectively prevent CBMs from mixing concepts together. The results for Clevr in Appendix B paint a similar picture.

6 Related Work

Shortcuts in machine learning. Shortcuts occur when machine learning models solve a prediction task by using features that correlate with but do not cause the desired output, leading to poor OOD behavior [Geirhos et al., 2020, Teso et al., 2023, Ye et al., 2024, Steinmann et al., 2024a]. The shortcuts literature however focuses on black-box models rather than CBMs. Existing studies on the semantics of CBM concepts [Margeloiu et al.,

⁵For Clevr, we focus on representative CBMs with high fit on the training data.

2021, Mahinpei et al., 2021, Havasi et al., 2022, Raman et al., 2023] focus on individual failures but propose no well-defined, formal notion of intended semantics. One exception is [Marconato et al., 2023a] which however, like other works, ignores the role of the inference layer. We build on known results on reasoning shortcuts [Li et al., 2023, Marconato et al., 2023b, Wang et al., 2023, Umili et al., 2024] which are restricted to NeSy-CBMs in which the prior knowledge is given and fixed. Our analysis upgrades these results to general CBMs. Furthermore, our simulations indicate that strategies that are effective for CBMs and RSs no longer work for JRSs. At the same time, while NeSy approaches that learn the prior knowledge and concepts jointly are increasingly popular [Wang et al., 2019, Yang et al., 2020, Liu et al., 2023, Daniele et al., 2023, Tang and Ellis, 2023, Wüst et al., 2024], existing work neglects the issue of shortcuts in this setting. Our work partially fills this gap.

Relation to identifiability. Works in Independent Component Analysis and Causal Representation Learning focus on the identifiability of representations up to an equivalence relation, typically up to permutations and rescaling [Khemakhem et al., 2020a, Gresele et al., 2020, von Kügelgen et al., 2024] or more general transformations [Roeder et al., 2021, Buchholz et al., 2022]. The equivalence relation introduced along with intended semantics (Definition 3.3) establishes a specific connection between the maps α and β . This aligns with existing works that aim to identify representations and linear inference layers using supervised labels [Lachapelle et al., 2023, Fumero et al., 2023, Bing et al., 2023]. Taeb et al. [2022] studied the identifiability of a VAE-based CBM with continuous-valued concepts. In contrast, we provide an analysis of a broader class of (NeSy) CBMs commonly used in practice. Moreover, while prior works primarily focus on identifying continuous-valued representations, we examine the identifiability of *discrete* concepts *and* of the inference layer. [Rajendran et al., 2024] explores the identifiability of (potentially discrete) concepts linearly encoded in model representations but is limited to a multi-environment setting, not including supervised labels. Our results differ in that we show how concepts can be identified in CBMs by circumventing joint reasoning shortcuts.

7 Conclusion

We study the issue of learning CBMs and NeSy-CBMs with high-quality quality concepts and inference layers. To this end, we formalize intended semantics and joint reasoning shortcuts (JRSs), show how reducing the number *deterministic* JRSs to zero provably prevents *all* JRSs, yielding identifiability, and investigate natural mitigation strategies. Numerical simulations indicate that JRSs are very frequent and impactful, and that the only (partially) beneficial mitigation is contrastive learning. Our analysis aims to pave the way to the design of effective solutions and therefore more robust and interpretable CBMs.

In future work, we plan to extend our theory to concept learning in general neural nets and large language models. Moreover, we will take a closer look at more complex mitigations such as techniques for smartly constraining the inference layer [Liu et al., 2023, Wüst et al., 2024], debiasing [Bahadori and Heckerman, 2021], and interaction with human experts [Teso et al., 2023].

Acknowledgements

The authors are grateful to Antonio Vergari, Emile van Krieken and Luigi Gresele for useful discussions. Funded by the European Union. Views and opinions expressed are however those of the author(s) only and do not necessarily reflect those of the European Union or the European Health and Digital Executive Agency (HaDEA). Neither the European Union nor the granting authority can be held responsible for them. Grant Agreement no. 101120763 - TANGO

References

- Kareem Ahmed, Stefano Teso, Kai-Wei Chang, Guy Van den Broeck, and Antonio Vergari. Semantic Probabilistic Layers for Neuro-Symbolic Learning. In *NeurIPS*, 2022.
- David Alvarez-Melis and Tommi S Jaakkola. Towards robust interpretability with self-explaining neural networks. In *NeurIPS*, 2018.
- Mohammad Taha Bahadori and David Heckerman. Debiasing concept-based explanations with causal analysis. In *ICLR*, 2021.
- Pierre Baldi. Autoencoders, unsupervised learning, and deep architectures. In *ICML Workshop on Unsupervised and Transfer Learning*, 2012.
- Simon Bing, Jonas Wahl, Urmi Ninad, and Jakob Runge. Invariance & causal representation learning: Prospects and limitations. In *Causal Representation Learning Workshop at NeurIPS 2023*, 2023.

- Samuele Bortolotti et al. A benchmark suite for systematically evaluating reasoning shortcuts. In *NeurIPS Datasets & Benchmarks Track*, 2024.
- Simon Buchholz, Michel Besserve, and Bernhard Schölkopf. Function classes for identifiable nonlinear independent component analysis. *Advances in Neural Information Processing Systems*, 35:16946–16961, 2022.
- Rich Caruana. Multitask learning. *Machine learning*, 1997.
- Supratik Chakraborty, Kuldeep S. Meel, and Moshe Y. Vardi. Algorithmic improvements in approximate counting for probabilistic inference: From linear to logarithmic sat calls. In *IJCAI*, 2016.
- Oscar Chang, Lampros Flokas, Hod Lipson, and Michael Spranger. Assessing satnet’s ability to solve the symbol grounding problem. *NeurIPS*, 2020.
- Chaofan Chen, Oscar Li, Daniel Tao, Alina Barnett, Cynthia Rudin, and Jonathan K Su. This looks like that: Deep learning for interpretable image recognition. *NeurIPS*, 2019.
- Ting Chen, Simon Kornblith, Mohammad Norouzi, and Geoffrey Everest Hinton. A simple framework for contrastive learning of visual representations. 2020a.
- Zhi Chen, Yijie Bei, and Cynthia Rudin. Concept whitening for interpretable image recognition. *Nature Machine Intelligence*, 2020b.
- Alessandro Daniele, Tommaso Campari, Sagar Malhotra, and Luciano Serafini. Deep symbolic learning: discovering symbols and rules from perceptions. In *IJCAI*, 2023.
- Luc De Raedt and Angelika Kimmig. Probabilistic (logic) programming concepts. *Machine Learning*, 100: 5–47, 2015.
- David Debot, Pietro Barbiero, Francesco Giannini, Gabriele Ciravegna, Michelangelo Diligenti, and Giuseppe Marra. Interpretable concept-based memory reasoning. In *NeurIPS*, 2024.
- Aaron Defazio and Samy Jelassi. Adaptivity without compromise: A momentumized, adaptive, dual averaged gradient method for stochastic optimization, 2021. URL <https://arxiv.org/abs/2101.11075>.
- Michelangelo Diligenti, Marco Gori, Marco Maggini, and Leonardo Rigutini. Bridging logic and kernel machines. *Machine learning*, 86(1):57–88, 2012.
- Gabriele Dominici, Pietro Barbiero, Francesco Giannini, Martin Gjoreski, and Marc Langheinrich. Anybms: How to turn any black box into a concept bottleneck model. *arXiv preprint arXiv:2405.16508*, 2024.
- Ivan Donadello, Luciano Serafini, and Artur D’Avila Garcez. Logic tensor networks for semantic image interpretation. In *IJCAI*, 2017.
- Mateo Espinosa Zarlenga, Pietro Barbiero, Gabriele Ciravegna, Giuseppe Marra, Francesco Giannini, Michelangelo Diligenti, Frederic Precioso, Stefano Melacci, Adrian Weller, Pietro Lio, et al. Concept embedding models. In *NeurIPS 2022-36th Conference on Neural Information Processing Systems*, 2022.
- Mateo Espinosa Zarlenga, Katie Collins, Krishnamurthy Dvijotham, Adrian Weller, Zohreh Shams, and Mateja Jamnik. Learning to receive help: Intervention-aware concept embedding models. *NeurIPS*, 2024.
- Marco Fumero, Florian Wenzel, Luca Zancato, Alessandro Achille, Emanuele Rodolà, Stefano Soatto, Bernhard Schölkopf, and Francesco Locatello. Leveraging sparse and shared feature activations for disentangled representation learning. *Advances in Neural Information Processing Systems*, 36:27682–27698, 2023.
- Robert Geirhos, Jörn-Henrik Jacobsen, Claudio Michaelis, Richard Zemel, Wieland Brendel, Matthias Bethge, and Felix A Wichmann. Shortcut learning in deep neural networks. *Nature Machine Intelligence*, 2(11): 665–673, 2020.
- Eleonora Giunchiglia and Thomas Lukasiewicz. Coherent hierarchical multi-label classification networks. *NeurIPS*, 2020.
- Luigi Gresele, Paul K Rubenstein, Arash Mehrjou, Francesco Locatello, and Bernhard Schölkopf. The incomplete rosetta stone problem: Identifiability results for multi-view nonlinear ica. In *Uncertainty in Artificial Intelligence*, pages 217–227. PMLR, 2020.
- Luigi Gresele, Julius Von Kügelgen, Vincent Stimper, Bernhard Schölkopf, and Michel Besserve. Independent mechanism analysis, a new concept? *Advances in neural information processing systems*, 34:28233–28248, 2021.
- Avani Gupta and PJ Narayanan. A survey on concept-based approaches for model improvement. *arXiv preprint arXiv:2403.14566*, 2024.

- Marton Havasi, Sonali Parbhoo, and Finale Doshi-Velez. Addressing leakage in concept bottleneck models. 2022.
- Geoffrey Hinton. Distilling the knowledge in a neural network. *arXiv preprint arXiv:1503.02531*, 2015.
- Nick Hoernle, Rafael Michael Karampatsis, Vaishak Belle, and Kobi Gal. Multiplexnet: Towards fully satisfied logical constraints in neural networks. In *AAAI*, 2022.
- Lei Huang, Weijiang Yu, Weitao Ma, Weihong Zhong, Zhangyin Feng, Haotian Wang, Qianglong Chen, Weihua Peng, Xiaocheng Feng, Bing Qin, et al. A survey on hallucination in large language models: Principles, taxonomy, challenges, and open questions. *ACM Transactions on Information Systems*, 2024.
- Glenn Jocher, Jing Qiu, and Ayush Chaurasia. Ultralytics YOLO, January 2023. URL <https://github.com/ultralytics/ultralytics>.
- Justin Johnson, Bharath Hariharan, Laurens Van Der Maaten, Li Fei-Fei, C Lawrence Zitnick, and Ross Girshick. Clevr: A diagnostic dataset for compositional language and elementary visual reasoning. In *CVPR*, 2017.
- Ilyes Khemakhem, Diederik Kingma, Ricardo Monti, and Aapo Hyvarinen. Variational autoencoders and nonlinear ica: A unifying framework. In *AISTATS*, 2020a.
- Ilyes Khemakhem, Ricardo Monti, Diederik Kingma, and Aapo Hyvarinen. Ice-beem: Identifiable conditional energy-based deep models based on nonlinear ica. *Advances in Neural Information Processing Systems*, 33: 12768–12778, 2020b.
- Eunji Kim, Dahuin Jung, Sangha Park, Siwon Kim, and Sungroh Yoon. Probabilistic concept bottleneck models. In *International Conference on Machine Learning*, pages 16521–16540. PMLR, 2023.
- Diederik P Kingma. Auto-encoding variational bayes. *arXiv preprint arXiv:1312.6114*, 2013.
- Diederik P Kingma. Adam: A method for stochastic optimization. *arXiv preprint arXiv:1412.6980*, 2014.
- Pang Wei Koh, Thao Nguyen, Yew Siang Tang, Stephen Mussmann, Emma Pierson, Been Kim, and Percy Liang. Concept bottleneck models. In *International conference on machine learning*, pages 5338–5348. PMLR, 2020.
- Harold W Kuhn. The hungarian method for the assignment problem. *Naval research logistics quarterly*, 1955.
- Sebastien Lachapelle, Tristan Deleu, Divyat Mahajan, Ioannis Mitliagkas, Yoshua Bengio, Simon Lacoste-Julien, and Quentin Bertrand. Synergies between disentanglement and sparsity: Generalization and identifiability in multi-task learning. In *ICML*, 2023.
- Balaji Lakshminarayanan, Alexander Pritzel, and Charles Blundell. Simple and scalable predictive uncertainty estimation using deep ensembles. *Advances in neural information processing systems*, 30, 2017.
- Yann LeCun. The mnist database of handwritten digits. <http://yann.lecun.com/exdb/mnist/>, 1998.
- Piyawat Lertvittayakumjorn, Lucia Specia, and Francesca Toni. Find: human-in-the-loop debugging deep text classifiers. In *Conference on Empirical Methods in Natural Language Processing*, pages 332–348, 2020.
- Oscar Li, Hao Liu, Chaofan Chen, and Cynthia Rudin. Deep learning for case-based reasoning through prototypes: A neural network that explains its predictions. In *AAAI*, 2018.
- Zenan Li, Zehua Liu, Yuan Yao, Jingwei Xu, Taolue Chen, Xiaoxing Ma, L Jian, et al. Learning with logical constraints but without shortcut satisfaction. In *ICLR*, 2023.
- Phillip Lippe, Sara Magliacane, Sindy Löwe, Yuki M Asano, Taco Cohen, and Efstratios Gavves. Biscuit: Causal representation learning from binary interactions. In *Uncertainty in Artificial Intelligence*, pages 1263–1273. PMLR, 2023.
- Marco Lippi and Paolo Frasconi. Prediction of protein β -residue contacts by markov logic networks with grounding-specific weights. *Bioinformatics*, 2009.
- Anji Liu, Hongming Xu, Guy Van den Broeck, and Yitao Liang. Out-of-distribution generalization by neural-symbolic joint training. In *Proceedings of the AAAI Conference on Artificial Intelligence*, volume 37, pages 12252–12259, 2023.
- Anita Mahinpei, Justin Clark, Isaac Lage, Finale Doshi-Velez, and Weiwei Pan. Promises and pitfalls of black-box concept learning models. In *International Conference on Machine Learning: Workshop on Theoretic Foundation, Criticism, and Application Trend of Explainable AI*, volume 1, pages 1–13, 2021.
- Robin Manhaeve, Sebastijan Dumancic, Angelika Kimmig, Thomas Demeester, and Luc De Raedt. Deep-ProbLog: Neural Probabilistic Logic Programming. *NeurIPS*, 2018.

- Robin Manhaeve, Sebastijan Dumančić, Angelika Kimmig, Thomas Demeester, and Luc De Raedt. Neural probabilistic logic programming in deepproblog. *Artificial Intelligence*, 298:103504, 2021.
- Ričards Marcinkevičs, Sonia Laguna, and Moritz VandenHirtz. Beyond concept bottleneck models: How to make black boxes intervenable? In *NeurIPS*, 2024.
- Emanuele Marconato, Andrea Passerini, and Stefano Teso. Glancenets: Interpretable, leak-proof concept-based models. *Advances in Neural Information Processing Systems*, 35:21212–21227, 2022.
- Emanuele Marconato, Andrea Passerini, and Stefano Teso. Interpretability is in the mind of the beholder: A causal framework for human-interpretable representation learning. *Entropy*, 2023a.
- Emanuele Marconato, Stefano Teso, Antonio Vergari, and Andrea Passerini. Not all neuro-symbolic concepts are created equal: Analysis and mitigation of reasoning shortcuts. In *NeurIPS*, 2023b.
- Emanuele Marconato, Samuele Bortolotti, Emile van Krieken, Antonio Vergari, Andrea Passerini, and Stefano Teso. BEARS Make Neuro-Symbolic Models Aware of their Reasoning Shortcuts. *Uncertainty in AI*, 2024.
- Andrei Margeloiu, Matthew Ashman, Umang Bhatt, Yanzhi Chen, Mateja Jamnik, and Adrian Weller. Do concept bottleneck models learn as intended? *arXiv preprint arXiv:2105.04289*, 2021.
- Guido Montúfar, Johannes Rauh, and Nihat Ay. On the fisher metric of conditional probability polytopes. *Entropy*, 2014.
- Paolo Morettin, Andrea Passerini, and Roberto Sebastiani. A unified framework for probabilistic verification of ai systems via weighted model integration. *arXiv preprint arXiv:2402.04892*, 2024.
- Jason Morton. Relations among conditional probabilities. *Journal of Symbolic Computation*, 50:478–492, 2013.
- Tuomas Oikarinen, Subhro Das, Lam M Nguyen, and Tsui-Wei Weng. Label-free concept bottleneck models. In *ICLR*, 2022.
- Eleonora Poeta, Gabriele Ciravegna, Eliana Pastor, Tania Cerquitelli, and Elena Baralis. Concept-based explainable artificial intelligence: A survey. *arXiv preprint arXiv:2312.12936*, 2023.
- Goutham Rajendran, Simon Buchholz, Bryon Aragam, Bernhard Schölkopf, and Pradeep Kumar Ravikumar. From causal to concept-based representation learning. In *The Thirty-eighth Annual Conference on Neural Information Processing Systems*, 2024.
- Naveen Raman, Mateo Espinosa Zarlenga, Juyeon Heo, and Mateja Jamnik. Do concept bottleneck models obey locality? In *XAI in Action: Past, Present, and Future Applications*, 2023.
- Geoffrey Roeder, Luke Metz, and Durk Kingma. On linear identifiability of learned representations. In *International Conference on Machine Learning*, pages 9030–9039. PMLR, 2021.
- Emanuele Sansone and Robin Manhaeve. Learning Symbolic Representations Through Joint Generative and DIscriminative Training. In *IJCAI 2023 Workshop on Knowledge-Based Compositional Generalization*, 2023.
- Yoshihide Sawada and Keigo Nakamura. Concept bottleneck model with additional unsupervised concepts. *IEEE Access*, 10:41758–41765, 2022.
- Simon Schrodi, Julian Schur, Max Argus, and Thomas Brox. Concept bottleneck models without predefined concepts. *arXiv preprint arXiv:2407.03921*, 2024.
- Gesina Schwalbe. Concept embedding analysis: A review. *arXiv preprint arXiv:2203.13909*, 2022.
- Sungbin Shin, Yohan Jo, Sungsoo Ahn, and Namhoon Lee. A closer look at the intervention procedure of concept bottleneck models. In *ICML*, 2023.
- Hikaru Shindo, Viktor Pfanschilling, Devendra Singh Dhami, and Kristian Kersting. (alpha)ilp: thinking visual scenes as differentiable logic programs. *Machine Learning*, 112(5):1465–1497, 2023.
- Divyansh Srivastava, Ge Yan, and Tsui-Wei Weng. VLG-CBM: Training concept bottleneck models with vision-language guidance. In *NeurIPS*, 2024.
- Wolfgang Stammer, Patrick Schramowski, and Kristian Kersting. Right for the Right Concept: Revising Neuro-Symbolic Concepts by Interacting with their Explanations. In *Proceedings of the IEEE/CVF Conference on Computer Vision and Pattern Recognition*, pages 3619–3629, 2021.
- David Steinmann, Felix Divo, Maurice Kraus, Antonia Wüst, Lukas Struppek, Felix Friedrich, and Kristian Kersting. Navigating shortcuts, spurious correlations, and confounders: From origins via detection to mitigation. *arXiv preprint arXiv:2412.05152*, 2024a.

- David Steinmann, Wolfgang Stammer, Felix Friedrich, and Kristian Kersting. Learning to intervene on concept bottlenecks. In *ICML*, 2024b.
- Zechen Sun, Yisheng Xiao, Juntao Li, Yixin Ji, Wenliang Chen, and Min Zhang. Exploring and mitigating shortcut learning for generative large language models. In *LREC-COLING*, 2024.
- Armeen Taeb, Nicolo Ruggeri, Carina Schnuck, and Fanny Yang. Provable concept learning for interpretable predictions using variational autoencoders, 2022.
- Hao Tang and Kevin Ellis. From perception to programs: regularize, overparameterize, and amortize. In *ICML*, 2023.
- Stefano Teso, Öznur Alkan, Wolfgang Stammer, and Elizabeth Daly. Leveraging explanations in interactive machine learning: An overview. *Frontiers in AI*, 2023.
- Elena Umili, Francesco Argenziano, and Roberto Capobianco. Neural reward machines. In *ECAI 2024*, pages 3055–3062. Ios Press, 2024.
- Emile van Krieken, Thiviyan Thanapalasingam, Jakub M Tomczak, Frank van Harmelen, and Annette ten Teije. A-nesi: A scalable approximate method for probabilistic neurosymbolic inference. *arXiv preprint arXiv:2212.12393*, 2022.
- Julius Von Kügelgen, Yash Sharma, Luigi Gresele, Wieland Brendel, Bernhard Schölkopf, Michel Besserve, and Francesco Locatello. Self-supervised learning with data augmentations provably isolates content from style. *Advances in neural information processing systems*, 34:16451–16467, 2021.
- Julius von Kügelgen, Michel Besserve, Liang Wendong, Luigi Gresele, Armin Kekić, Elias Bareinboim, David Blei, and Bernhard Schölkopf. Nonparametric identifiability of causal representations from unknown interventions. *Advances in Neural Information Processing Systems*, 36, 2024.
- Kaifu Wang, Efi Tsamoura, and Dan Roth. On learning latent models with multi-instance weak supervision. In *NeurIPS*, 2023.
- Po-Wei Wang, Priya Donti, Bryan Wilder, and Zico Kolter. Satnet: Bridging deep learning and logical reasoning using a differentiable satisfiability solver. In *International Conference on Machine Learning*, pages 6545–6554. PMLR, 2019.
- Zhenzhen Wang, Aleksander Popel, and Jeremias Sulam. Cbm-zero: Concept bottleneck model with zero performance loss. 2024.
- Antonia Wüst, Wolfgang Stammer, Quentin Delfosse, Devendra Singh Dhami, and Kristian Kersting. Pix2code: Learning to compose neural visual concepts as programs. *arXiv preprint arXiv:2402.08280*, 2024.
- Xuan Xie, Kristian Kersting, and Daniel Neider. Neuro-symbolic verification of deep neural networks. In *IJCAI*, 2022.
- Jingyi Xu, Zilu Zhang, Tal Friedman, Yitao Liang, and Guy Broeck. A semantic loss function for deep learning with symbolic knowledge. In *ICML*, 2018.
- Xiao-Wen Yang, Wen-Da Wei, Jie-Jing Shao, Yu-Feng Li, and Zhi-Hua Zhou. Analysis for abductive learning and neural-symbolic reasoning shortcuts. In *ICML*, 2024a.
- Yu Yang, Eric Gan, Gintare Karolina Dziugaite, and Baharan Mirzasoleiman. Identifying spurious biases early in training through the lens of simplicity bias. In *AISTATS*, 2024b.
- Yue Yang, Artemis Panagopoulou, Shenghao Zhou, Daniel Jin, Chris Callison-Burch, and Mark Yatskar. Language in a bottle: Language model guided concept bottlenecks for interpretable image classification. In *CVPR*, 2023.
- Zhun Yang, Adam Ishay, and Joohyung Lee. Neurasp: Embracing neural networks into answer set programming. In *IJCAI 2020*, 2020.
- Wenqian Ye, Guangtao Zheng, Xu Cao, Yunsheng Ma, and Aidong Zhang. Spurious correlations in machine learning: A survey. *arXiv preprint arXiv:2402.12715*, 2024.
- Mert Yuksekogonul, Maggie Wang, and James Zou. Post-hoc concept bottleneck models. *arXiv preprint arXiv:2205.15480*, 2022.
- Lotfi Asker Zadeh. Fuzzy logic. *Computer*, 1988.
- Faried Abu Zaid, Dennis Diekmann, and Daniel Neider. Distribution-aware neuro-symbolic verification. *AISoLA*, pages 445–447, 2023.
- Mateo Espinosa Zarlenga, Pietro Barbiero, Zohreh Shams, Dmitry Kazhdan, Umang Bhatt, Adrian Weller, and Mateja Jamnik. Towards robust metrics for concept representation evaluation. In *AAAI*, 2023.

A Implementation Details

Here, we provide additional details about metrics, datasets, and models, for reproducibility. All the experiments were implemented using Python 3.9 and Pytorch 1.13 and run on one A100 GPU. The implementations of DPL, and the code for RSs mitigation strategies were taken verbatim from [Marconato et al., 2023b], while the code for DSL was taken from [Daniele et al., 2023]. DPL* and bears* were implement on top of DSL codebase.

A.1 Datasets

All data sets were generated using the rsbench library [Bortolotti et al., 2024].

A.1.1 MNIST-Add

MNIST-Add [Manhaeve et al., 2018] consists of pairs of MNIST digits [LeCun, 1998], ranging from 0 to 9, and the goal is to predict their sum. The prior knowledge used for generating the labels is simply the rule of addition: $K = (Y = C_1 + C_2)$. This task does not admit RSs nor JRSs when digits are processed separately. Below we report four examples:

$$\{((0, 1), 1), ((5, 8), 13), ((6, 6), 12), ((4, 1), 5)\} \quad (9)$$

All splits cover all possible pairs of concepts, from (0, 0) to (9, 9), i.e., there is no sampling bias. Overall, MNIST-Add has 42, 000 training examples, 12, 000 validation examples, and 6, 000 test examples.

A.2 MNIST-SumParity

Similarly, in MNIST-SumParity the goal is to predict the *parity* of the sum, i.e., the prior knowledge is the rule: $K = (Y = (C_1 + C_2) \bmod 2)$. This task is more challenging for our purposes, as it is affected by both RSs and JRSs, cf. Fig. 1. Below we report four examples:

$$\{((0, 1), 1), ((5, 8), 1), ((6, 6), 0), ((4, 1), 1)\} \quad (10)$$

We consider two variants: like MNIST-Add, in MNIST-SumParity proper the training and test splits contain all possible combinations of digits, while in *biased* MNIST-SumParity the training set contains (even, even), (odd, odd) and (odd, even) pairs, while the test set contains (even, odd) pairs. This fools CBMs into learning an incorrect inference layer implementing subtraction instead of addition-and-parity, as illustrated in Fig. 1. Both variants have the same number of training, validation, and test examples as MNIST-Add.

A.3 Clevr

Clevr [Johnson et al., 2017] consists of 3D scenes of simple objects rendered with Blender, see Fig. 4. Images are $3 \times 128 \times 128$ and contain a variable number of objects. We consider only images with 2 to 4 objects each, primarily due to scalability issues with DPL. The ground-truth labels were computed by applying the rules (prior knowledge) proposed by [Stammer et al., 2021], reported in Table 6. Objects are entirely determined by four concepts, namely shape, color, material, and size. We list all possible values in Table 5. Overall, Clevr has 6000 training examples, 1200 validation examples, and 1800 test examples.

| Property | Value |
|-----------|--|
| Shapes | Cube, Sphere, Cylinder |
| Colors | Gray Red, Blue, Green, Brown, Purple, Cyan, Yellow |
| Materials | Rubber, Metal |
| Sizes | Large, Small |

Table 5: Clevr properties.

| Class | Condition |
|---------|---|
| Class 1 | $\exists x_1 (\text{Cube}(x_1) \wedge \text{Large}(x_1))$ $\wedge \exists x_2 (\text{Cylinder}(x_2) \wedge \text{Large}(x_2))$ |
| Class 2 | $\exists x_1 (\text{Cube}(x_1) \wedge \text{Small}(x_1) \wedge \text{Metal}(x_1))$ $\wedge \exists x_2 (\text{Sphere}(x_2) \wedge \text{Small}(x_2))$ |
| Class 3 | $\exists x_1 (\text{Sphere}(x_1) \wedge \text{Large}(x_1) \wedge \text{Blue}(x_1))$ $\wedge \exists x_2 (\text{Sphere}(x_2) \wedge \text{Small}(x_2) \wedge \text{Yellow}(x_2))$ |

Table 6: Clevr classes.

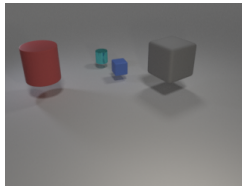


Figure 4: Example of Clevr data.

Preprocessing. All CBMs process objects separately. Following [Shindo et al., 2023], we fine-tune a pretrained YoloV11 model [Jocher et al., 2023] (for 10 epochs, random seed 13) on a subset of the training set’s bounding boxes, and use it to predict bounding boxes for all images. For each training and test image, we concatenate the regions in the bounding boxes, obtaining a list 2 to 4 images which plays the role of input for our CBMs.

Each object has $8 \times 3 \times 2 \times 2 = 96$ possible configurations of concept values, and we handle between 2 and 4 objects, hence the inference layer has to model $96^2 + 96^3 + 96^4$ distinct possibilities. Due to the astronomical

number of possibilities (which would entail a huge truth table/inference layer for DSL and related CBMs), we split the inference layer in two: we first predict individual concepts, and then we aggregate them (into, e.g., `large-cube` and `small-yellow-sphere`) and use these for prediction. Despite this simplification, `Clevr` still induces JRSs in learned CBMs.

A.4 Metrics

For all models, we report the metrics averaged over *five random seeds*.

Label quality. We measure the macro average F_1 -score and Accuracy, to account for class imbalance.

Concept quality. We compute concept quality via Accuracy and F_1 -score. However, the order of ground-truth and predicted concepts might differ, e.g., in `Clevr` G_1 might represent whether “color = red”, while C_1 whether “color = blue”. Therefore, in order to compute these metrics we have to first align them using the Hungarian matching algorithm using concept-wise Pearson correlation on the test data [Kuhn, 1955]. The algorithm computes the correlation matrix R between \mathbf{g} and \mathbf{c} , i.e., $R_{ij} = \text{corr}(G_i, C_j)$ where corr is the correlation coefficient, and then infers a permutation π between concept values (e.g., mapping ground-truth color “red” to predicted value “blue”) that maximizes the above objective. The metrics are computed by comparing the reordered ground-truth annotations with the predicted concepts.

Inference layer quality. The same permutation is also used to assess knowledge quality. Specifically, we apply it to reorder the ground-truth concepts and then feed these to the learned inference layer, evaluating the accuracy and F_1 score of the resulting predictions.

For `MNIST-Add` and `MNIST-SumParity`, we conducted an exhaustive evaluation since the number of possible combinations to supervise is 100. The results in [Table 1](#) and [Table 2](#) evaluate the knowledge exhaustively, whereas in [Table 4](#), we separately assess the knowledge of in-distribution and out-of-distribution combinations.

In `Clevr`, as discussed in [Appendix A.3](#), there are too many combinations of concept values to possibly evaluate them all. Therefore, both supervision and evaluation are performed by randomly sampling 100 combinations of ground-truth concepts.

A.5 Architectures

For `MNIST-SumParity` and `MNIST-Add`, We employed the architectures from [Bortolotti et al., 2024], while for `DSL`, `DPL*`, and `bears*`, we followed the architecture described in [Daniele et al., 2023]. For `Clevr` instead, we adopted the decoder presented in [Table 7](#) and the encoder presented in [Table 8](#). All models process different objects (e.g., digits) separately using the same backbone.

Table 7: Encoder architecture for `Clevr`.

| INPUT | LAYER TYPE | PARAMETER | OUTPUT |
|----------------|-------------------|--------------------------------------|--------------|
| (128, 128, 3) | Convolution | depth=32, kernel=3, stride=1, pad=1 | ReLU |
| (128, 128, 32) | MaxPool2d | kernel=2, stride=2 | |
| (64, 64, 32) | Convolution | depth=64, kernel=3, stride=1, pad=1 | ReLU |
| (64, 64, 64) | MaxPool2d | kernel=2, stride=2 | |
| (64, 32, 32) | Convolution | depth=128, kernel=3, stride=1, pad=1 | ReLU |
| (128, 32, 32) | AdaptiveAvgPool2d | out=(1, 1) | |
| (128, 1, 1) | Flatten | | |
| (128) | Linear | dim=40, bias = True | \mathbf{c} |
| (128) | Linear | dim=640, bias = True | μ |
| (128) | Linear | dim=640, bias = True | σ |

Table 8: Decoder architecture for `Clevr`

| INPUT | LAYER TYPE | PARAMETER | ACTIVATION |
|---------------|-----------------|--------------------------------------|------------|
| (255) | Linear | dim=32768, bias = True | |
| (8, 8, 512) | ConvTranspose2d | depth=256, kernel=4, stride=2, pad=1 | |
| (16, 16, 256) | BatchNorm2d | | ReLU |
| (16, 16, 256) | ConvTranspose2d | depth=128, kernel=4, stride=2, pad=1 | |
| (32, 32, 128) | BatchNorm2d | | ReLU |
| (32, 32, 128) | ConvTranspose2d | depth=64, kernel=4, stride=2, pad=1 | |
| (64, 64, 64) | BatchNorm2d | | ReLU |
| (64, 64, 64) | ConvTranspose2d | depth=3, kernel=4, stride=2, pad=1 | Tanh |

Details of CBNM. For `Clevr`, we used a standard linear layer. Since this is not expressive enough for `MNIST-Add` and `MNIST-SumParity`, we replaced it with an interpretable second-degree polynomial layer, i.e., it associates

weights to *combinations of two predicted digits* rather than individual digits. We also include a small entropy term, which empirically facilitates data fit when little or no concept supervision is available.

Details of SENN. SENN [Alvarez-Melis and Jaakkola, 2018] are unsupervised concept-based models consisting of a neural network that produces a distribution over concepts, a neural network that assigns a score to those concepts, and a decoder. The final prediction is made by computing the dot product between the predicted concepts and their predicted scores. SENN by default includes a reconstruction penalty, a robustness loss, and a sparsity term.

In our implementation, we focus only on the reconstruction penalty. The robustness loss, which aims to make the relevance scores Lipschitz continuous, requires computing Jacobians, making the training of those models infeasible in terms of computational time and resources. Additionally, we did not implement the sparsity term, as it conflicts with the quality of concepts we aim to study.

Details of bears*. bears* combines DSL [Daniele et al., 2023] and BEARS [Marconato et al., 2024]. BEARS is a NeSy architectures based on deep ensembles [Lakshminarayanan et al., 2017], designed to improve the calibration of NeSy models in the presence of RSs and provide uncertainty estimation for concepts that may be affected by such RSs and it assumes to be given prior knowledge.

Since in our setup the inference layer is learned, we built an ensemble with one learnable inference layer as in DSL and multiple concept extractors. The first element of the ensemble learns both the concepts and the inference layer. Then, we freeze it and train the other concept extractors using the frozen inference layer for prediction. In this sense, bears* provides awareness of the reasoning shortcuts present in the knowledge learned by the first model.

A.6 Mitigation Strategies

Concept supervision. When evaluating mitigation strategies, concept supervision for MNIST-SumParity was incrementally supplied for two more concepts at each step, following this order: 3, 4, 1, 0, 2, 8, 9, 5, 6, 7. For Clevr, supervision was specifically provided for sizes, shapes, materials, and colors, in this order.

Knowledge distillation. This was implemented using a cross-entropy on the inference layer. For DSL and DPL, ground-truth concepts were fed into the learned truth table, expecting the correct label. Similarly, for CBNMs, which use a linear layer, the same approach was applied. In evaluating the mitigation strategies, we supervised all possible combinations for MNIST-Add, whereas for Clevr, we supervised a maximum of 500 randomly sampled combinations.

Entropy maximization. The entropy regularization term follows the implementation in [Marconato et al., 2023b]. The loss is defined as $1 - \frac{1}{k} \sum_{i=1}^k H_{m_i} [p_\theta(c_i)]$ where $p_\theta(C)$ represents the marginal distribution over the concepts, and H_{m_i} is the normalized Shannon entropy over m_i possible values of the distribution.

Reconstruction. The reconstruction penalty is the same as in [Marconato et al., 2023b]. In this case, the concept extractor outputs both concepts c and style variables z , i.e., it implements a distribution $p_\theta(c, z|x) = p_\theta(c|x) \cdot p_\theta(z|x)$. The reconstruction penalty is defined as: $-\mathbb{E}_{(c,z) \sim p_\theta(c,z|x)} [\log p_\psi(x|c, z)]$ where $p_\psi(x|c, z)$ represents the decoder network.

Contrastive loss. We implemented contrastive learning using the InfoNCE loss, comparing the predicted *concept distribution* of the current batch with that of its respective augmentations. Following the recommendations of Chen et al. [2020a], we applied the following augmentations to each batch: random cropping (20 pixels for MNIST and 125 pixels for Clevr), followed by resizing, color jittering, and Gaussian blur.

A.7 Model Selection

Optimization. For DPL*, bears*, CBNM and SENN we used the Adam optimizer [Kingma, 2014], while for DSL and DPL we achieved better results using the Madgrad optimizer [Defazio and Jelassi, 2021].

Hyperparameter search. We performed an extensive grid search on the validation set over the following hyperparameters: (i) Learning rate (γ) in $\{1e-4, 1e-3, 1e-2\}$; (ii) Weight decay (ω) in $\{0, 1e-4, 1e-3, 1e-2, 1e-1\}$; (iii) Reconstruction, contrastive loss, entropy loss, concept supervision loss and knowledge supervision loss weights ($w_r, w_c, w_h, w_{c_{sup}}$ and w_k , respectively) in $\{0.1, 1, 2, 5, 8, 10\}$; (iv) Batch size (ν) in $\{32, 64, 128, 256, 512\}$. DSL and DPL* have additional hyperparameters for the truth table: ε_{sym} and ε_{rul} for DSL, and λ_r , the truth table learning rate, for DPL*.

All experiments were run for approximately 50 epochs for MNIST variants and 100 epochs for Clevr using early stopping based on validation set $F_1(Y)$ performance. The exponential decay rate β was set to 0.99 for all experiments, as we empirically found it to provide the best performance across tasks. In all experiments, we selected $\gamma = 1e - 3$.

To answer the first research question in [Section 5](#) on MNIST-Add, for DPL we used: $\nu = 32$ and $\omega = 0.0001$; for DSL: $\nu = 128$, $\omega = 0.001$, $\varepsilon_{sym} = 0.2807344052335263$, and $\varepsilon_{rul} = 0.107711951632426$; for CBNM: $\nu = 256$ and $\omega = 0.0001$; for DPL*: $\nu = 32$, $\omega = 0.01$, and $\lambda_r = 0.0001$; for SENN: $\nu = 64$, $\omega = 0.001$, and $w_r = 0.1$; while for bears* we set the diversification loss term to 0 and the entropy term to 0.1. On MNIST-SumParity and its biased version, for DPL we used: $\nu = 512$ and $\omega = 0.0001$; for DSL: $\nu = 128$, $\omega = 0.0001$, $\varepsilon_{sym} = 0.2807344052335263$, and $\varepsilon_{rul} = 0.107711951632426$; for CBNM: $\nu = 256$ and $\omega = 0.0001$; for DPL*: $\nu = 32$, $\omega = 0.01$, and $\lambda_r = 0.01$; for SENN: $\nu = 64$, $\omega = 0.001$, and $w_r = 0.1$; while for bears* we set the diversification loss term to 0.1 and the entropy term to 0.2. On Clevr, for DPL, CBNM, and DPL*, we used $\nu = 32$ and $\omega = 0.001$; for DPL*, $\lambda_r = 0.001$.

For the second research question, we performed a grid search for each mitigation strategy individually. Additionally, since our analysis focuses on optimal models, we trained multiple models and retained only those achieving optimal $F_1(Y)$ performance on the validation set. For MNIST-SumParity, we set $\nu = 128$, $\omega = 0.001$, and $w_{csup} = 1$ across all experiments. For specific mitigation strategies, we used $w_h = 1$ for entropy regularization, $w_r = 0.01$ for reconstruction, $w_c = 0.1$ for contrastive learning, and $w_k = 1$ for knowledge supervision. For Clevr, we applied the same settings: $\nu = 128$, $\omega = 0.001$, and $w_{csup} = 1$ for all experiments. The specific mitigation strategy weights were set as follows: $w_h = 1$ for entropy regularization, $w_r = 1$ for reconstruction, $w_c = 0.1$ for contrastive learning, and $w_k = 1$ for knowledge supervision. When concept supervision is applied, we follow a sequential training approach as in [\[Koh et al., 2020\]](#). During the initial epochs, the model learns only the concepts, and later, it jointly optimizes both the concepts and the label, as they are challenging to learn simultaneously.

B Additional results

B.1 Full Results for the Case Studies

We report additional results for **Q1** including additional models and metrics – namely label accuracy Acc_Y , concept accuracy Acc_C , and inference layer accuracy $Acc(\beta)$, and negative log-likelihood on the test set. The two additional models are: “CBNM noent”, like CBNM except it does not include any entropy term; and CBNM₂₀ which is a regular CBNM for which 20% of the concept values (e.g., two digits in MNIST-based tasks) receive full concept supervision.

Table 9: Complete results for MNIST-Add.

| METHOD | Acc_Y | $F_1(Y)$ | Acc_C | $F_1(C)$ | $Cls(C) (\downarrow)$ | $F_1(\beta)$ | $Acc(\beta)$ | NLL |
|--------------------------|-----------------|-----------------|-----------------|-----------------|-----------------------|-----------------|-----------------|-----------------|
| DPL | 0.98 ± 0.01 | 0.98 ± 0.01 | 0.99 ± 0.01 | 0.99 ± 0.01 | 0.01 ± 0.01 | – | – | 0.17 ± 0.03 |
| CBNM | 0.98 ± 0.01 | 0.98 ± 0.01 | 0.99 ± 0.01 | 0.99 ± 0.01 | 0.01 ± 0.01 | 1.00 ± 0.01 | 1.00 ± 0.01 | 0.11 ± 0.01 |
| CBNM noent | 0.98 ± 0.01 | 0.98 ± 0.01 | 0.80 ± 0.10 | 0.74 ± 0.13 | 0.08 ± 0.04 | 0.37 ± 0.09 | 0.42 ± 0.06 | 0.26 ± 0.01 |
| CBNM ₂₀ | 0.98 ± 0.01 | 0.98 ± 0.01 | 0.99 ± 0.01 | 0.99 ± 0.01 | 0.01 ± 0.01 | 0.67 ± 0.02 | 0.59 ± 0.02 | 0.70 ± 0.02 |
| CBNM ₂₀ noent | 0.92 ± 0.02 | 0.94 ± 0.01 | 0.60 ± 0.09 | 0.48 ± 0.10 | 0.22 ± 0.12 | 0.02 ± 0.01 | 0.12 ± 0.02 | 1.09 ± 0.01 |
| DSL | 0.96 ± 0.02 | 0.96 ± 0.02 | 0.98 ± 0.01 | 0.98 ± 0.01 | 0.01 ± 0.01 | 1.00 ± 0.01 | 1.00 ± 0.01 | 0.38 ± 0.14 |
| DPL* | 0.90 ± 0.09 | 0.91 ± 0.09 | 0.93 ± 0.07 | 0.92 ± 0.08 | 0.01 ± 0.01 | 0.90 ± 0.08 | 0.90 ± 0.09 | 0.02 ± 0.01 |
| bears* | 0.81 ± 0.12 | 0.76 ± 0.15 | 0.87 ± 0.12 | 0.87 ± 0.13 | 0.01 ± 0.01 | 0.67 ± 0.14 | 0.65 ± 0.10 | 0.34 ± 0.22 |
| SENN | 0.97 ± 0.01 | 0.97 ± 0.01 | 0.84 ± 0.05 | 0.80 ± 0.07 | 0.01 ± 0.01 | 0.75 ± 0.08 | 0.75 ± 0.08 | 0.01 ± 0.01 |

Table 10: Complete results for MNIST-SumParity.

| METHOD | Acc_Y | $F_1(Y)$ | Acc_C | $F_1(C)$ | $Cls(C) (\downarrow)$ | $F_1(\beta)$ | $Acc(\beta)$ | NLL |
|------------|-----------------|-----------------|-----------------|-----------------|-----------------------|-----------------|-----------------|-----------------|
| DPL | 0.99 ± 0.01 | 0.99 ± 0.01 | 0.47 ± 0.04 | 0.43 ± 0.08 | 0.36 ± 0.15 | – | – | 0.33 ± 0.01 |
| CBNM | 0.90 ± 0.18 | 0.90 ± 0.18 | 0.21 ± 0.06 | 0.09 ± 0.03 | 0.66 ± 0.09 | 0.54 ± 0.04 | 0.21 ± 0.06 | 0.52 ± 1.04 |
| CBNM noent | 0.98 ± 0.01 | 0.98 ± 0.01 | 0.22 ± 0.01 | 0.08 ± 0.02 | 0.72 ± 0.13 | 0.53 ± 0.09 | 0.53 ± 0.09 | 0.07 ± 0.02 |
| DSL | 0.94 ± 0.03 | 0.94 ± 0.03 | 0.20 ± 0.01 | 0.07 ± 0.01 | 0.80 ± 0.01 | 0.52 ± 0.01 | 0.51 ± 0.02 | 0.29 ± 0.16 |
| DPL* | 0.99 ± 0.01 | 0.99 ± 0.01 | 0.22 ± 0.01 | 0.07 ± 0.01 | 0.80 ± 0.01 | 0.50 ± 0.05 | 0.50 ± 0.06 | 0.06 ± 0.01 |
| bears* | 0.99 ± 0.01 | 0.99 ± 0.01 | 0.28 ± 0.05 | 0.30 ± 0.03 | 0.22 ± 0.04 | 0.36 ± 0.09 | 0.37 ± 0.09 | 0.04 ± 0.01 |
| SENN | 0.99 ± 0.01 | 0.99 ± 0.01 | 0.53 ± 0.05 | 0.49 ± 0.05 | 0.01 ± 0.01 | 0.53 ± 0.06 | 0.53 ± 0.06 | 0.01 ± 0.01 |

Table 11: Complete Results for MNIST-SumParity biased.

| METHOD | Acc_Y | $F_1(Y)$ | Acc_C | $F_1(C)$ | $Cls(C) (\downarrow)$ | $F_1(\beta)$ | $Acc(\beta)$ | NLL |
|--------------------------|-----------------|-----------------|-----------------|-----------------|-----------------------|-----------------|-----------------|-----------------|
| DPL | 0.99 ± 0.01 | 0.99 ± 0.01 | 0.65 ± 0.05 | 0.59 ± 0.06 | 0.08 ± 0.07 | – | – | 0.06 ± 0.01 |
| CBNM noent | 0.99 ± 0.01 | 0.99 ± 0.01 | 0.22 ± 0.01 | 0.08 ± 0.02 | 0.76 ± 0.06 | 0.52 ± 0.04 | 0.52 ± 0.04 | 0.05 ± 0.01 |
| CBNM ₂₀ | 0.99 ± 0.01 | 0.99 ± 0.01 | 0.21 ± 0.01 | 0.07 ± 0.01 | 0.80 ± 0.01 | 0.51 ± 0.01 | 0.52 ± 0.01 | 0.07 ± 0.04 |
| CBNM ₂₀ noent | 0.99 ± 0.01 | 0.99 ± 0.01 | 0.22 ± 0.01 | 0.07 ± 0.01 | 0.80 ± 0.01 | 0.49 ± 0.04 | 0.48 ± 0.04 | 0.04 ± 0.01 |
| DSL | 0.94 ± 0.03 | 0.94 ± 0.03 | 0.20 ± 0.01 | 0.07 ± 0.01 | 0.80 ± 0.01 | 0.02 ± 0.01 | 0.09 ± 0.02 | 0.29 ± 0.16 |
| bears* | 0.99 ± 0.01 | 0.99 ± 0.01 | 0.20 ± 0.01 | 0.07 ± 0.01 | 0.78 ± 0.04 | 0.48 ± 0.04 | 0.49 ± 0.04 | 0.03 ± 0.01 |

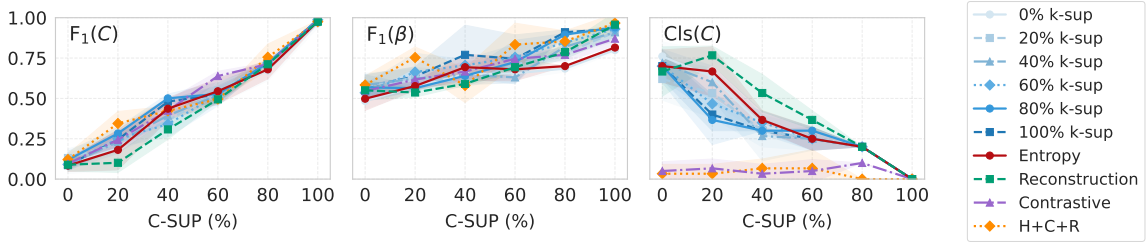


Figure 5: Fig. 3 with standard deviation over 5 seeds

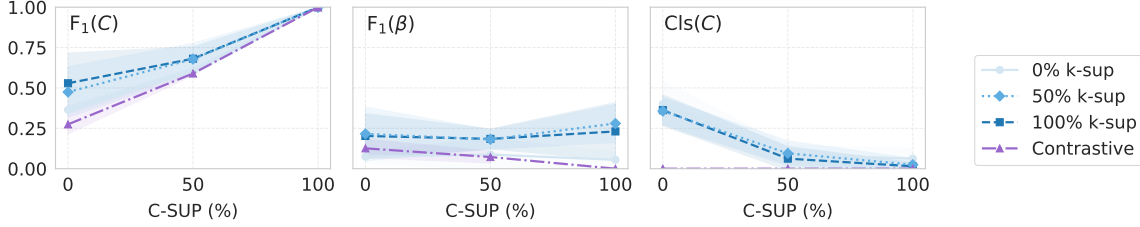


Figure 6: Mitigation strategies evaluated for CBNM on Clevr, with standard deviation over 5 seeds. We evaluated only the contrastive strategy as it performed best. Since supervising all knowledge is infeasible, we observe that for sampled configurations (leading to out-of-distribution settings), the learned knowledge does not generalize.

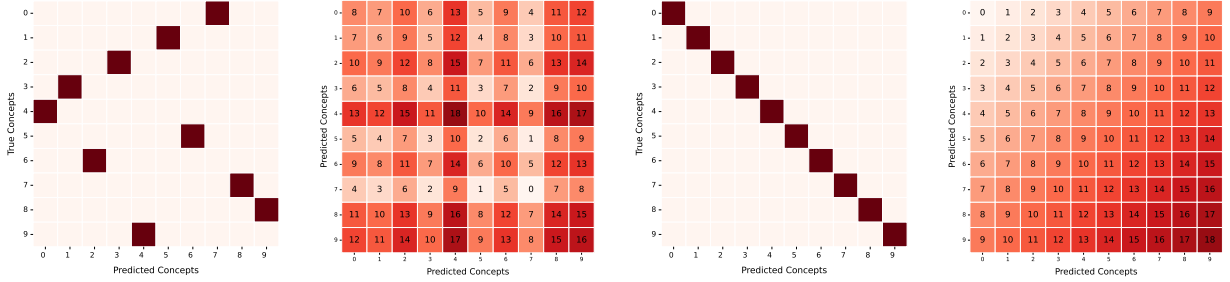


Figure 7: Confusion matrices of concepts for CBNM on MNIST-Add (first row: before alignment, second row: after alignment) along with the corresponding knowledge: number in cells refer to the predicted sum.

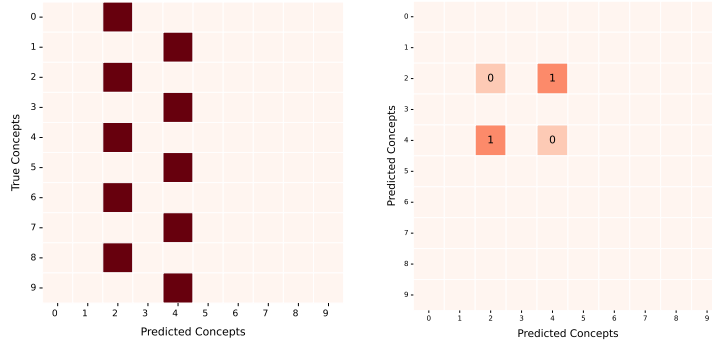


Figure 8: Concepts and inference layer learned by CBNM on MNIST-SumParity before (two left) and after (two right) the post-hoc alignment step. For concepts, we report the confusion matrix. For the inference layer, we visualize the learned operation as a truth table: numbers within cells indicate the label predicted for each combination of predicted digits.

B.2 Number of Reasoning Shortcuts and Joint Reasoning Shortcuts

Here, we report the approximate number of deterministic reasoning shortcuts and joint reasoning shortcuts for MNIST-Add and MNIST-SumParity. We obtained these numbers by extending the count-rss software included in rsbench [Bortolotti et al., 2024] to the enumeration of JRSs, compatibly with Eq. (8) and Eq. (7).

We considered downsized versions of both MNIST-Add and MNIST-SumParity, with input digits restricted to the range $\{0, \dots, N\}$, and resorted to the approximate model counter approxMC [Chakraborty et al., 2016] for obtaining approximate counts in the hardest cases. All counts assume object independence is in place (i.e., that the two input digits are processed separately), for simplicity. The situation is similar when this is not the case, except that the all counts grow proportionally.

The number of RSs and JRSs for increasing N are reported in Table 12. Specifically, the #RSs column indicates the number of regular RSs obtained by fixing the prior knowledge (that is, assuming $\beta = \beta^*$) and

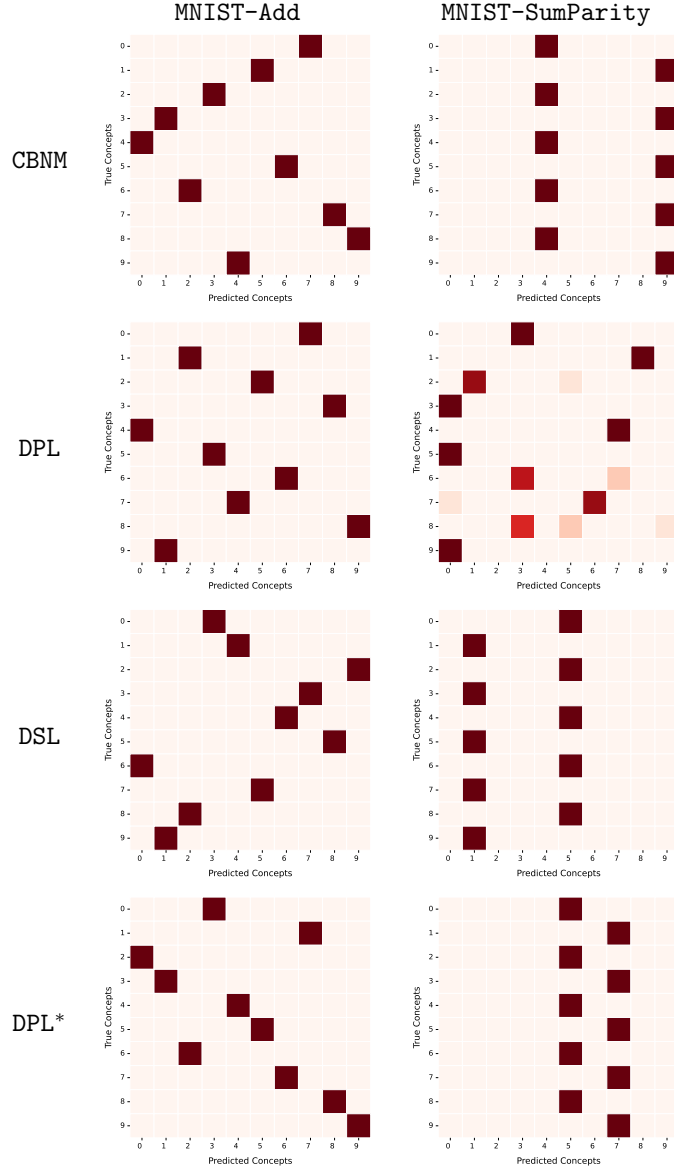


Figure 9: Confusion matrices between ground-truth and predicted concepts. In MNIST-SumParity models tend to favor α 's that collapse concepts together, hinting at simplicity bias.

matches the count in [Marconato et al., 2023b] for the same tasks. The #JRSs columns refer to the CBM case, where the inference layer is learned from data (i.e., β might not match β^*). We report two distinct counts for JRSs: one assumes that β 's that match on all concepts actively output by α should be considered identical despite possible differences on “inactive” concepts that α predicts as constant (#JRSs non-redundant) or not (# JRSs).

As can be seen from the results, JRSs quickly outnumber regular RSs as N grows, as anticipated in Section 3.1. This suggests that, as expected, learning CBMs with intended semantics by optimizing label likelihood is more challenging when prior knowledge is not given *a priori*.

Table 12: Number of RSs vs. JRSs in MNIST-SumParity.

| N | #RSs | #JRSs | #JRSs (non-redundant) |
|-----|-------------------------------|----------------------------------|-------------------------------|
| 3 | $(1.10 \pm 0.00) \times 10^1$ | $(3.84 \pm 0.60) \times 10^2$ | $(1.20 \pm 0.00) \times 10^1$ |
| 4 | $(6.30 \pm 0.00) \times 10^1$ | $(1.11 \pm 0.05) \times 10^5$ | $(1.27 \pm 0.06) \times 10^2$ |
| 5 | $(3.70 \pm 0.15) \times 10^2$ | $(1.16 \pm 0.05) \times 10^8$ | $(1.40 \pm 0.70) \times 10^3$ |
| 6 | $(2.98 \pm 0.10) \times 10^3$ | $(4.45 \pm 0.19) \times 10^{11}$ | $(1.74 \pm 0.13) \times 10^4$ |
| 7 | $(2.56 \pm 0.26) \times 10^4$ | $(8.08 \pm 0.33) \times 10^{15}$ | $(2.61 \pm 0.14) \times 10^5$ |
| 8 | $(2.62 \pm 0.15) \times 10^5$ | $(5.39 \pm 0.25) \times 10^{20}$ | $(4.21 \pm 0.10) \times 10^6$ |

C Theoretical Material

In this section, we start by summarizing the prerequisite material. We begin by recalling a central Lemma proven in [Marconato et al., 2023b] that allows us to write the condition for likelihood-optimal models in terms of α . To ease of comparison, let $p(\mathbf{C} | \mathbf{X}) := \mathbf{f}(\mathbf{X})$ and $p(\mathbf{Y} | \mathbf{X}) := (\omega \circ \mathbf{f})(\mathbf{X})$ denote the conditional distributions defined by the CBM $(\mathbf{f}, \omega) \in \mathcal{F} \times \Omega$, and:

$$p(\mathbf{Y} | \mathbf{G}) := \mathbb{E}_{\mathbf{x} \sim p^*(\mathbf{X} | \mathbf{G})} [p(\mathbf{Y} | \mathbf{x})] \quad (11)$$

Also, we consider the following joint distributions:

$$p^*(\mathbf{X}, \mathbf{Y}) = p^*(\mathbf{Y} | \mathbf{X})p^*(\mathbf{X}), \quad p(\mathbf{X}, \mathbf{Y}) = p(\mathbf{Y} | \mathbf{X})p^*(\mathbf{X}) \quad (12)$$

Lemma C.1 ([Marconato et al., 2023b]). *It holds that: (i) The true risk of p can be upper bounded as follows:*

$$\mathbb{E}_{(\mathbf{x}, \mathbf{y}) \sim p^*(\mathbf{X}, \mathbf{Y})} [\log p(\mathbf{y} | \mathbf{x})] = -\text{KL}[p^*(\mathbf{X}; \mathbf{Y}) \parallel p(\mathbf{X}, \mathbf{Y})] - H[p^*(\mathbf{X}, \mathbf{Y})] \quad (13)$$

$$\leq \mathbb{E}_{\mathbf{g} \sim p(\mathbf{G})} (-\text{KL}[p^*(\mathbf{Y} | \mathbf{g}; \mathbf{K}) \parallel p(\mathbf{Y} | \mathbf{g})] - H[p^*(\mathbf{Y} | \mathbf{g}; \mathbf{K})]) \quad (14)$$

where KL is the Kullback-Leibler divergence and H is the Shannon entropy. Moreover, under [Assumptions 3.1](#) and [3.2](#), $p(\mathbf{Y} | \mathbf{X}; \mathbf{K})$ is an optimum of the LHS of [Eq. \(14\)](#) if and only if $p(\mathbf{Y} | \mathbf{G})$ is an optimum of the RHS. (ii) There exists a bijection between the deterministic concept distributions $p(\mathbf{C} | \mathbf{X})$ that, for each $\mathbf{g} \in \text{supp}(\mathbf{G})$, are constant over the support of $p^*(\mathbf{X} | \mathbf{g})$ apart for zero-measure subspaces $\mathcal{X}^0 \subset \text{supp}(p^*(\mathbf{X} | \mathbf{g}))$ and the deterministic distributions of the form $p(\mathbf{C} | \mathbf{G})$.

Here, point (i) connects the optima of the likelihood $p(\mathbf{Y} | \mathbf{X})$ and the optima of $p(\mathbf{Y} | \mathbf{G})$. This implies that, under [Assumptions 3.1](#) and [3.2](#), knowing the optima of $p(\mathbf{Y} | \mathbf{G})$ informs us about optimal CBMs $p(\mathbf{Y} | \mathbf{X})$. Notice that, to a single $\alpha(\mathbf{G}) = p(\mathbf{C} | \mathbf{G})$ might correspond to multiple choices of $\mathbf{f} \in \mathcal{F}$. The choice is unique if, by point (ii), we consider deterministic $p(\mathbf{C} | \mathbf{G})$ showing that they are into one-to-one correspondence with $p(\mathbf{C} | \mathbf{X})$ that are almost constant in the support.

Limiting to those α 's in point (ii), we can find a simple way to describe optima for $p(\mathbf{Y} | \mathbf{G})$.

Lemma C.2 (Deterministic optima of the likelihood). *Under [Assumptions 3.1](#) and [3.2](#), for all CBMs $(\mathbf{f}, \omega) \in \mathcal{F} \times \Omega$ where $\mathbf{f} : \mathbf{x} \mapsto \mathbf{c}$ is constant over the support of $p^*(\mathbf{X} | \mathbf{g})$ apart for a zero-measure subspace $\mathcal{X}^0 \subset \text{supp}(p^*(\mathbf{X} | \mathbf{g}))$, for all $\mathbf{g} \in \mathcal{G}$, it holds that the optima of the likelihood for $p(\mathbf{Y} | \mathbf{G})$ are obtained when:*

$$\forall \mathbf{g} \in \text{supp}(p^*(\mathbf{G})), (\beta \circ \alpha)(\mathbf{g}) = \beta^*(\mathbf{g}) \quad (15)$$

where $\alpha(\mathbf{g}) := \mathbb{E}_{\mathbf{x} \sim p^*(\mathbf{X} | \mathbf{g})} [\mathbf{f}(\mathbf{x})] \in \text{Vert}(\mathcal{A})$ and $\beta(\mathbf{c}) := \omega(\mathbb{1}\{\mathbf{C} = \mathbf{c}\}) \in \text{Vert}(\mathcal{B})$.

Proof. Notice that by [Lemma C.1](#), it holds that $\alpha \in \text{Vert}(\mathcal{A})$ is a deterministic conditional distribution. Since $\mathbf{f} : \mathbf{x} \rightarrow \mathbf{c}$ is constant over all $\mathbf{x} \sim p^*(\mathbf{X} | \mathbf{g})$ for a fixed $\mathbf{g} \in \mathcal{G}$, it holds that $\mathbf{f}(\mathbf{x}) = \alpha(\mathbf{g})$ apart for some \mathbf{x} in a measure-zero subspace $\mathcal{X}^0 \subset \text{supp}(p^*(\mathbf{X} | \mathbf{g}))$, therefore we get:

$$\mathbb{E}_{\mathbf{x} \sim p^*(\mathbf{X} | \mathbf{g})} [\omega(\mathbf{f}(\mathbf{x}))] = \omega(\alpha(\mathbf{g})) \quad (16)$$

$$= (\beta \circ \alpha)(\mathbf{g}) \quad (17)$$

where in the last line we substituted ω with β since α is deterministic. For $p(\mathbf{Y} | \mathbf{G})$, the necessary and sufficient condition for maximum log-likelihood is:

$$\forall \mathbf{g} \in \text{supp}(p^*(\mathbf{G})), p(\mathbf{Y} | \mathbf{g}) = \beta^*(\mathbf{g}) \quad (18)$$

and substituting [Eq. \(17\)](#) we get:

$$\forall \mathbf{g} \in \text{supp}(p^*(\mathbf{G})), (\beta \circ \alpha)(\mathbf{g}) = \beta^*(\mathbf{g}) \quad (19)$$

showing the claim. \square

C.1 Equivalence relation given by [Definition 3.3](#)

We start by proving that [Definition 3.3](#) defines an equivalence relation.

Proposition C.3. *[Definition 3.3](#) defines an equivalence relation (denoted as \sim) between couples $(\alpha, \beta), (\alpha', \beta') \in \mathcal{A} \times \mathcal{B}$, where $(\alpha, \beta) \sim (\alpha', \beta')$ if there exist a permutation $\pi : [k] \rightarrow [k]$ and k element-wise invertible functions ψ_1, \dots, ψ_k such that:*

$$\forall \mathbf{g} \in \mathcal{G}, \alpha(\mathbf{g}) = (\mathbf{P}_\pi \circ \psi \circ \alpha')(\mathbf{g}) \quad (20)$$

$$\forall \mathbf{c} \in \mathcal{C}, \beta(\mathbf{c}) = (\beta' \circ \psi^{-1} \circ \mathbf{P}_\pi^{-1})(\mathbf{c}) \quad (21)$$

where $\mathbf{P}_\pi : \mathcal{C} \rightarrow \mathcal{C}$ is the permutation matrix induced by π and $\psi(\mathbf{c}) := (\psi_1(c_1), \dots, \psi_k(c_k))$.

Proof. To the aim of the proof, it is useful to analyze how \mathbf{P}_π and ψ relate. Consider for any $\mathbf{c} \in \mathcal{C}$:

$$(\mathbf{P}_\pi \circ \psi)(\mathbf{c}) = \mathbf{P}_\pi(\psi_1(c_1), \dots, \psi_k(c_k)) \quad (22)$$

$$= (\psi_{\pi(1)}(c_{\pi(1)}), \dots, \psi_{\pi(k)}(c_{\pi(k)})) \quad (23)$$

Denoting with $\psi_\pi(\mathbf{c}) := (\psi_{\pi(1)}(c_1), \dots, \psi_{\pi(k)}(c_k))$, we have that:

$$(\mathbf{P}_\pi \circ \psi)(\mathbf{c}) = (\psi_\pi \circ \mathbf{P}_\pi)(\mathbf{c}) \quad (24)$$

From this expression, notice it holds for all $\mathbf{c} \in \mathcal{C}$:

$$(\mathbf{P}_\pi \circ \psi)(\mathbf{c}) = (\mathbf{P}_\pi \circ \psi \circ \mathbf{P}_\pi^{-1} \circ \mathbf{P}_\pi)(\mathbf{c}) \quad (25)$$

$$(\psi_\pi \circ \mathbf{P}_\pi)(\mathbf{c}) = ((\mathbf{P}_\pi \circ \psi \circ \mathbf{P}_\pi^{-1}) \circ \mathbf{P}_\pi)(\mathbf{c}) \quad (26)$$

so that we can equivalently write $\psi_\pi := \mathbf{P}_\pi \circ \psi \circ \mathbf{P}_\pi^{-1}$.

Reflexivity. This follows by choosing $\mathbf{P}_\pi = \text{id}$ and similarly $\psi_i = \text{id}$ for all $i \in [k]$.

Symmetry. We have to prove that $(\alpha, \beta) \sim (\alpha', \beta') \implies (\alpha', \beta') \sim (\alpha, \beta)$. To this end, we start by taking the expression for α in terms of α' . Consider for any $\mathbf{g} \in \mathcal{G}$:

$$\alpha(\mathbf{g}) = (\mathbf{P}_\pi \circ \psi \circ \alpha')(\mathbf{g}) \quad (27)$$

$$= (\psi_\pi \circ \mathbf{P}_\pi \circ \alpha')(\mathbf{g}) \quad (28)$$

where in the last step we used [Eq. \(24\)](#). By first inverting ψ_π and then \mathbf{P}_π , we obtain that:

$$\alpha'(\mathbf{g}) = (\mathbf{P}_\pi^{-1} \circ \psi_\pi^{-1} \circ \alpha)(\mathbf{g}) \quad (29)$$

showing the reflexivity of α . With similar steps, we can show that a similar relation also holds for β' , that is for all $\mathbf{c} \in \mathcal{C}$:

$$\beta'(\mathbf{c}) = (\beta \circ \psi_\pi \circ \mathbf{P}_\pi)(\mathbf{c}) \quad (30)$$

Transitivity. We have to prove that if $(\alpha, \beta) \sim (\alpha', \beta')$ and $(\alpha', \beta') \sim (\alpha^\dagger, \beta^\dagger)$ then also $(\alpha, \beta) \sim (\alpha^\dagger, \beta^\dagger)$. We start from the expression of α and α' , where we have that $\forall \mathbf{g} \in \mathcal{G}$:

$$\alpha(\mathbf{g}) = (\mathbf{P}_\pi \circ \psi \circ \alpha')(\mathbf{g}) \quad (31)$$

$$\alpha'(\mathbf{g}) = (\mathbf{P}_{\pi'} \circ \psi' \circ \alpha^\dagger)(\mathbf{g}) \quad (32)$$

We proceed by substituting the expression of α' in α to obtain:

$$\alpha(\mathbf{g}) = (\mathbf{P}_\pi \circ \psi \circ \mathbf{P}_{\pi'} \circ \psi' \circ \alpha^\dagger)(\mathbf{g}) \quad (33)$$

$$= (\mathbf{P}_\pi \circ \mathbf{P}_{\pi'} \circ \mathbf{P}_{\pi'}^{-1} \circ \psi \circ \mathbf{P}_{\pi'} \circ \psi' \circ \alpha^\dagger)(\mathbf{g}) \quad (\text{Composing } \mathbf{P}_\pi \text{ with the identity } \mathbf{P}_{\pi'} \circ \mathbf{P}_{\pi'}^{-1})$$

$$= (\mathbf{P}_\pi \circ \mathbf{P}_{\pi'} \circ \psi_{\pi'-1} \circ \psi' \circ \alpha^\dagger)(\mathbf{g}) \quad (\text{Using that } \psi_{\pi'-1} := \mathbf{P}_{\pi'}^{-1} \circ \psi \circ \mathbf{P}_{\pi'})$$

$$= (\mathbf{P}_{\pi^\dagger} \circ \psi^\dagger \circ \alpha^\dagger)(\mathbf{g}) \quad (34)$$

where we defined $\mathbf{P}_{\pi^\dagger} := \mathbf{P}_\pi \circ \mathbf{P}_{\pi'}$ and $\psi^\dagger := \psi_{\pi'-1} \circ \psi'$. With similar steps, we obtain that β can be related to β^\dagger as:

$$\beta(\mathbf{c}) = (\beta^\dagger \circ \psi^{\dagger-1} \circ \mathbf{P}_{\pi^\dagger}^{-1})(\mathbf{c}) \quad (35)$$

for all $\mathbf{c} \in \mathcal{C}$. This shows the equivalence relation of [Definition 3.3](#). \square

We now prove how solutions with intended semantics ([Definition 3.3](#)) relate to the optima of the log-likelihood:

Lemma C.4 (Intended semantics entails optimal models). *If a pair $(\alpha, \beta) \in \mathcal{A} \times \mathcal{B}$ possesses the intended semantics ([Definition 3.3](#)), it holds:*

$$\forall \mathbf{g} \in \mathcal{G}, (\beta \circ \alpha)(\mathbf{g}) = \beta^*(\mathbf{g}) \quad (36)$$

Proof. We make use of the fact that by [Definition 3.3](#) it holds:

$$\alpha(\mathbf{g}) = (\mathbf{P}_\pi \circ \psi \circ \text{id})(\mathbf{g}) \quad (37)$$

$$\beta(\mathbf{c}) = (\beta^* \circ \psi^{-1} \circ \mathbf{P}_\pi^{-1})(\mathbf{c}) \quad (38)$$

Therefore, combining [Eqs. \(37\)](#) and [\(38\)](#) we get for all $\mathbf{g} \in \mathcal{G}$:

$$(\beta \circ \alpha)(\mathbf{g}) = (\beta^* \circ \mathbf{P}_\pi^{-1} \circ \psi^{-1} \circ \psi \circ \mathbf{P}_\pi)(\mathbf{g}) \quad (39)$$

$$= (\beta^* \circ \mathbf{P}_\pi^{-1} \circ \mathbf{P}_\pi)(\mathbf{g}) \quad (40)$$

$$= \beta^*(\mathbf{g}) \quad (41)$$

yielding the claim. \square

C.2 Proof of Theorem 3.5 and Corollary 3.6

Theorem C.5. Let $s\mathcal{G} := \bigcup_{i=1}^k \{|\mathcal{G}_i|\}$ be the set of cardinalities of each concept $G_i \subseteq \mathbf{G}$ and $ms\mathcal{G}$ denote the multi-set $ms\mathcal{G} := \{(|\mathcal{G}_i|, m(|\mathcal{G}_i|)), i \in [k]\}$, where $m(\bullet)$ denotes the multiplicity of each element of $s\mathcal{G}$. Under Assumptions 3.1 and 3.2, the number of deterministic JRSs $(\alpha, \beta) \in \text{Vert}(\mathcal{A}) \times \text{Vert}(\mathcal{B})$ amounts to:

$$\sum_{(\alpha, \beta) \in \text{Vert}(\mathcal{A}) \times \text{Vert}(\mathcal{B})} \mathbb{1}\left\{ \bigwedge_{\mathbf{g} \in \text{supp}(\mathbf{G})} (\beta \circ \alpha)(\mathbf{g}) = \beta^*(\mathbf{g}) \right\} - C[\mathcal{G}] \quad (42)$$

where $C[\mathcal{G}]$ is the total number of pairs with the intended semantics, given by $C[\mathcal{G}] := \prod_{\xi \in s\mathcal{G}} m(\xi)! \times \prod_{i=1}^k |\mathcal{G}_i|!$.

Proof. Since we are considering pairs $(\alpha, \beta) \in \text{Vert}(\mathcal{A}) \times \text{Vert}(\mathcal{B})$, we can stick to the fact that α defines a function $\alpha : \mathcal{G} \rightarrow \mathcal{C}$ and that, similarly, β defines a function $\beta : \mathcal{C} \rightarrow \mathcal{Y}$. In this case, $\beta \circ \alpha : \mathcal{G} \rightarrow \mathcal{Y}$ is a map from ground-truth concepts to labels. We start by Definition 3.3 and consider the pairs that attain maximum likelihood by Lemma C.2:

$$\forall \mathbf{g} \in \text{supp}(p^*(\mathbf{G})), (\beta \circ \alpha)(\mathbf{g}) = \beta^*(\mathbf{g}) \quad (43)$$

where, since $\alpha \in \text{Vert}(\mathcal{A})$ and is deterministic, we can substitute ω with β . Since both $\text{Vert}(\mathcal{A})$ and $\text{Vert}(\mathcal{B})$ are countable, we can convert this to a total count of pairs that attain maximum likelihood:

$$\sum_{(\alpha, \beta) \in \text{Vert}(\mathcal{A}) \times \text{Vert}(\mathcal{B})} \mathbb{1}\left\{ \bigwedge_{\mathbf{g} \in \text{supp}(p^*(\mathbf{G}))} (\beta \circ \alpha)(\mathbf{g}) = \beta^*(\mathbf{g}) \right\} \quad (44)$$

where, for each pair $(\alpha, \beta) \in \text{Vert}(\mathcal{A}) \times \text{Vert}(\mathcal{B})$ the sum increases by one if the condition of Eq. (43) is satisfied.

Among these optimal pairs, there are those possessing the intended semantics by Lemma C.4, which consists of possible permutations of the concepts and element-wise invertible transformations of the concept values. We start by evaluating the number of possible element-wise invertible transformations for each subset of concepts $\mathcal{G}_i \subset \mathcal{G}$.

Each concept c_i has values in the subset \mathcal{G}_i , for a total of $|\mathcal{G}_i|$ values. The overall number of possible invertible transformations is then given by the number of possible permutations, resulting in a total of $|\mathcal{G}_i|!$ maps. This means that the total number of element-wise invertible transformations is given by:

$$\prod_{i=1}^k |\mathcal{G}_i|! \quad (45)$$

Next, we consider what permutation of the concepts are possible. To this end, consider the set and the multi-set comprising all different \mathcal{G}_i cardinalities given by:

$$s\mathcal{G} := \bigcup_{i=1}^k \{|\mathcal{G}_i|\}, \quad ms\mathcal{G} := \{(|\mathcal{G}_i|, m(|\mathcal{G}_i|)) : i \in [k]\} \quad (46)$$

where $m(\bullet)$ counts how many repetitions are present. When the multi-set contains repeated numbers, i.e., when different c_i and c_j have the same cardinality, we have to account a possible permutation of the concept indices. Therefore, for each element $\xi \in s\mathcal{G}$ we have that the total number of permutations of concepts amount to:

$$\text{perm}(\mathcal{G}) := \prod_{\xi \in s\mathcal{G}} m(\xi)! \quad (47)$$

Finally, the total number of pairs possessing the intended semantics amount to $\text{perm}(\mathcal{G}) \times \prod_{i=1}^k |\mathcal{G}_i|!$, resulting that the total number of deterministic JRSs are:

$$\sum_{(\alpha, \beta) \in \text{Vert}(\mathcal{A}) \times \text{Vert}(\mathcal{B})} \mathbb{1}\left\{ \bigwedge_{\mathbf{g} \in \text{supp}(p^*(\mathbf{G}))} (\beta \circ \alpha)(\mathbf{g}) = \beta^*(\mathbf{g}) \right\} - \text{perm}(\mathcal{G}) \times \prod_{i=1}^k |\mathcal{G}_i|! \quad (48)$$

yielding the claim. \square

Corollary 3.6. Consider a fixed $\beta^* \in \text{Vert}(\mathcal{B})$. Under *Assumptions 3.1 and 3.2*, the number of deterministic JRSs $(\alpha, \beta^*) \in \text{Vert}(\mathcal{A}) \times \text{Vert}(\mathcal{B})$ is:

$$\sum_{\alpha \in \text{Vert}(\mathcal{A})} \mathbb{1}\{\bigwedge_{\mathbf{g} \in \text{supp}(\mathbf{G})} (\beta^* \circ \alpha)(\mathbf{g}) = \beta^*(\mathbf{g})\} - 1 \quad (8)$$

This matches the count for deterministic RSs in [Marconato et al., 2023b].

Proof. The proof follows immediately by replacing $\text{Vert}(\mathcal{B})$ with $\{\beta^*\}$, allowing only for the ground-truth inference function. In this context, by following similar steps of *Theorem 3.5*, we arrive at a similar count to *Eq. (44)*, that is:

$$\sum_{(\alpha, \beta) \in \text{Vert}(\mathcal{A}) \times \{\beta^*\}} \mathbb{1}\{\bigwedge_{\mathbf{g} \in \text{supp}(p^*(\mathbf{G}))} (\beta \circ \alpha)(\mathbf{g}) = \beta^*(\mathbf{g})\} \quad (49)$$

In the context of RSs, the only pair possessing the intended semantics is (id, β^*) , which has to be subtracted from *Eq. (49)*. This shows the claim. \square

C.3 Proof of Theorem 3.8

Theorem 3.8 (Identifiability). Under *Assumptions 3.1 and 3.2*, if the number of deterministic JRSs (*Eq. (7)*) is zero then every CBM $(\mathbf{f}, \omega) \in \mathcal{F} \times \Omega$ satisfying *Assumption 3.7* that attains maximum log-likelihood (*Eq. (4)*) possesses the intended semantics (*Definition 3.3*). That is, the pair $(\alpha, \beta) \in \mathcal{A} \times \mathcal{B}$ entailed by each such CBM is equivalent to the ground-truth pair (id, β^*) , i.e., $(\alpha, \beta) \sim (\text{id}, \beta^*)$.

Proof. Consider a pair $(\alpha, \beta) \in \mathcal{A} \times \mathcal{B}$, where both α and β can be non-deterministic conditional probability distributions. **Step (i).** We begin by first recalling *Lemma C.1*. Under *Assumptions 3.1 and 3.2*, a CBM $(\mathbf{f}, \omega) \in \mathcal{F} \times \Omega$ is optimal, i.e., it attains maximum likelihood, if it holds that:

$$\forall \mathbf{g} \in \text{supp}(p^*(\mathbf{G})), \mathbb{E}_{\mathbf{x} \sim p^*(\mathbf{x}|\mathbf{g})}[(\omega \circ \mathbf{f})(\mathbf{x})] = \beta^*(\mathbf{g}) \quad (50)$$

Notice that, according to *Assumptions 3.1 and 3.2*, it also holds that the labels must be predicted with probability one to attain maximum likelihood, that is:

$$\forall \mathbf{g} \in \mathcal{G}, \max \beta^*(\mathbf{g}) = 1 \quad (51)$$

Now consider a pair $(\alpha, \beta) \in \mathcal{A} \times \mathcal{B}$. By *Lemma C.1* (i), it holds that to obtain maximum likelihood, the learned knowledge $\beta : \mathcal{C} \rightarrow \Delta_{\mathcal{Y}}$ must be deterministic:

$$\max \beta(\mathbf{c}) = 1 \quad (52)$$

which implies that, necessarily, to have optimal β the space \mathcal{B} restricts to the set $\text{Vert}(\mathcal{B})$, so any learned knowledge $\beta \in \text{Vert}(\mathcal{B})$. This shows that optimal pairs (α, β) are in $\mathcal{A} \times \text{Vert}(\mathcal{B})$.

Step (ii). In this step, we make use of *Assumption 3.7* and consider only inference functions ω with that property. We start by considering a couple $(\mathbf{a}', \mathbf{b}') \in \text{Vert}(\mathcal{A}) \times \text{Vert}(\mathcal{B})$ that attain maximum likelihood, that is according to *Theorem 3.5*:

$$\forall \mathbf{g} \in \text{supp}(p^*(\mathbf{G})), (\mathbf{b}' \circ \mathbf{a}')(\mathbf{g}) = \beta^*(\mathbf{g}) \quad (53)$$

Now, we have to prove that, given $\mathbf{b}' \in \text{Vert}(\mathcal{B})$, there are no $\alpha \in \mathcal{A} \setminus \text{Vert}(\mathcal{A})$ that can attain maximum likelihood for at least one possible choice of $\omega' \in \Omega$, such that for all $\mathbf{c} \in \mathcal{C}$ it holds $\omega'(\mathbb{1}\{\mathbf{C} = \mathbf{c}\}) = \mathbf{b}'(\mathbf{c})$. Since \mathcal{A} is a simplex, we can always construct a non-deterministic conditional probability distribution $\alpha \in \mathcal{A}$ from a convex combination of the vertices $\mathbf{a}_i \in \text{Vert}(\mathcal{A})$, i.e., for all $\mathbf{g} \in \mathcal{G}$ it holds:

$$\alpha(\mathbf{g}) = \sum_{\alpha_i \in \text{Vert}(\mathcal{A})} \lambda_i \mathbf{a}_i(\mathbf{g}) \quad (54)$$

Consider another $\mathbf{a}'' \neq \mathbf{a}' \in \text{Vert}(\mathcal{A})$ and consider an arbitrary convex combination that defines a non-deterministic $\alpha \in \mathcal{A}$:

$$\forall \mathbf{g} \in \mathcal{G}, \alpha(\mathbf{g}) := \lambda \mathbf{a}'(\mathbf{g}) + (1 - \lambda) \mathbf{a}''(\mathbf{g}) \quad (55)$$

where $\lambda \in (0, 1)$. When the deterministic JRSs count (*Eq. (7)*) equals to zero, we know that by *Theorem 3.5* only $(\mathbf{a}', \mathbf{b}')$ attains maximum likelihood, whereas $(\mathbf{a}'', \mathbf{b}')$ is not optimal. Therefore, there exists at least one $\hat{\mathbf{g}} \in \text{supp}(p^*(\mathbf{G}))$ such that

$$(\beta' \circ \mathbf{a}')(\hat{\mathbf{g}}) \neq (\beta' \circ \mathbf{a}'')(\hat{\mathbf{g}}) \quad (56)$$

We now have to look at the form of \mathbf{f} that can induce such a non-deterministic $\alpha = \lambda \mathbf{a}' + (1 - \lambda) \mathbf{a}''$. Recalling, the definition of α (Eq. (2)) we have that:

$$\alpha(\mathbf{g}) = \mathbb{E}_{\mathbf{x} \sim p^*(\mathbf{X} | \mathbf{g})}[\mathbf{f}(\mathbf{x})] \quad (57)$$

$$= \lambda \mathbf{a}'(\mathbf{g}) + (1 - \lambda) \mathbf{a}''(\mathbf{g}) \quad (58)$$

For this α , there are two possible kinds of $\mathbf{f} \in \mathcal{F}$ that can express it.

(1) In one case, we can have $\mathbf{f} : \mathbb{R}^n \rightarrow \text{Vert}(\Delta_{\mathcal{C}})$ – mapping inputs to “hard” distributions over concepts. Since α is not a “hard” distribution (provided $\lambda \in (0, 1)$), $\mathbf{f}(\mathbf{x})$ must be equal to $\mathbf{a}'(\mathbf{g})$ for a fraction λ of the examples $\mathbf{x} \in \text{supp}(p^*(\mathbf{X} | \mathbf{g}))$ and to $\mathbf{a}''(\mathbf{g})$ for a fraction of $1 - \lambda$. In that case, it holds that there exist a subspace of non-vanishing measure $\mathcal{X}'' \subset \text{supp}(p^*(\mathbf{X} | \hat{\mathbf{g}}))$ such that $\mathbf{f}(\mathbf{x}) = \mathbf{a}''(\hat{\mathbf{g}})$. Therefore, for all $\mathbf{x} \in \mathcal{X}''$ we have that $(\mathbf{b}' \circ \mathbf{a}'')(\mathbf{x}) = (\omega \circ \mathbf{a}'')(\hat{\mathbf{g}}) \neq \beta^*(\hat{\mathbf{g}})$, and such an \mathbf{f} is suboptimal.

(2) The remaining option is that $\mathbf{f} : \mathbb{R}^n \rightarrow \Delta_{\mathcal{C}}$, excluding mapping to the vertices almost everywhere in $\text{supp}(p^*(\mathbf{X} | \hat{\mathbf{g}}))$. In light of this, we rewrite \mathbf{f} as follows:

$$\forall \mathbf{x} \in \text{supp}(p^*(\mathbf{X} | \hat{\mathbf{g}})), \mathbf{f}(\mathbf{x}) = \sum_{\mathbf{c} \in \mathcal{C}} p(\mathbf{c} | \mathbf{x}) \mathbb{1}\{\mathbf{C} = \mathbf{c}\} \quad (59)$$

where $p(\mathbf{c} | \mathbf{x}) := \mathbf{f}(\mathbf{x})_{\mathbf{c}}$. Let $\hat{\mathbf{c}}' := \mathbf{a}'(\hat{\mathbf{g}})$ and $\hat{\mathbf{c}}'' := \mathbf{a}''(\hat{\mathbf{g}})$. But α is a convex combination of \mathbf{a}' and \mathbf{a}'' , hence the function \mathbf{f} must attribute non-zero probability mass only to the concept vectors $\hat{\mathbf{c}}'$ and $\hat{\mathbf{c}}''$. Hence, we rewrite it as:

$$\forall \mathbf{x} \in \mathcal{X} \subseteq \text{supp}(p^*(\mathbf{X} | \hat{\mathbf{g}})), \mathbf{f}(\mathbf{x}) = p(\hat{\mathbf{c}}' | \mathbf{x}) \mathbb{1}\{\mathbf{C} = \hat{\mathbf{c}}'\} + p(\hat{\mathbf{c}}'' | \mathbf{x}) \mathbb{1}\{\mathbf{C} = \hat{\mathbf{c}}''\} \quad (60)$$

where \mathcal{X} has measure one. Notice that in this case it holds $\arg\max_{\mathbf{y} \in \mathcal{Y}} \mathbf{b}'(\hat{\mathbf{c}}')_{\mathbf{y}} \neq \arg\max_{\mathbf{y} \in \mathcal{Y}} \mathbf{b}'(\hat{\mathbf{c}}'')_{\mathbf{y}}$. By [Assumption 3.7](#) we have that, for any choice of $\lambda \in (0, 1)$ it holds that for all $\mathbf{x} \in \mathcal{X}$:

$$\begin{aligned} \max_{\mathbf{y} \in \mathcal{Y}} \omega(p(\hat{\mathbf{c}}' | \mathbf{x}) \mathbb{1}\{\mathbf{C} = \hat{\mathbf{c}}'\} + p(\hat{\mathbf{c}}'' | \mathbf{x}) \mathbb{1}\{\mathbf{C} = \hat{\mathbf{c}}''\}) &< \max(\arg\max_{\mathbf{y} \in \mathcal{Y}} \mathbf{b}'(\hat{\mathbf{c}}')_{\mathbf{y}}, \arg\max_{\mathbf{y} \in \mathcal{Y}} \mathbf{b}'(\hat{\mathbf{c}}'')_{\mathbf{y}}) \\ &\text{(Using the condition from Assumption 3.7)} \\ &= 1 \end{aligned} \quad (61)$$

where the last step in [Eq. \(61\)](#) follows from the fact that $\mathbf{b}' \in \text{Vert}(\mathcal{B})$, so giving point-mass conditional probability distributions.

(1) and (2) together show that any $\alpha \in \mathcal{A} \setminus \text{Vert}(\mathcal{A})$ constructed as a convex combination of \mathbf{a}' and an $\mathbf{a}'' \neq \mathbf{a}'$ cannot attain maximum likelihood. Hence, the optimal pairs restrict to $(\alpha, \beta) \in \text{Vert}(\mathcal{A}) \times \text{Vert}(\mathcal{B})$ and since the count of JRSs ([Eq. \(7\)](#)) is zero, all $(\alpha, \beta) \in \mathcal{A} \times \mathcal{B}$ that are optimal also possess the intended semantics. This concludes the proof. \square

D Impact of mitigation strategies on the deterministic JRSs count

We focus on how the count can be updated for some mitigation strategies that we accounted for in [Section 4](#). We consider those strategies that gives a constraint for the [Eq. \(7\)](#), namely: *multi-task learning*, *concept supervision*, *knowledge distillation*, and *reconstruction*.

D.1 Multi-task learning

Suppose that for a subset $\mathcal{G}^{\tau} \subseteq \text{supp}(p^*(\mathbf{G}))$, input examples are complemented with additional labels \mathbf{y}^{τ} , obtained by applying an inference layer $\beta_{\mathcal{K}^{\tau}}(\mathbf{g})$. Here, \mathcal{K}^{τ} represents the augmented knowledge, giving a set \mathcal{Y}^{τ} of additional labels. To understand how such a choice modifies the count of jrss, we have to consider those $\beta : \mathcal{C} \rightarrow \mathcal{Y} \times \mathcal{Y}^{\tau}$, where a component $\beta_{\mathcal{Y}}$ maps to the original task labels \mathcal{Y} and the other component $\beta_{\mathcal{Y}^{\tau}}$ maps to the augmented labels \mathcal{Y}^{τ} . Let $\mathcal{B}^* := \mathcal{B} \times \mathcal{B}^{\tau}$ the space where such functions are defined. As obtained in [[Marconato et al., 2023b](#)], the constraint for a pair $(\alpha, \beta) \in \text{Vert}(\mathcal{A}) \times \text{Vert}(\mathcal{B}^*)$ can be written as:

$$\mathbb{1}\{\bigwedge_{\mathbf{g} \in \mathcal{G}^{\tau}} (\beta_{\mathcal{Y}^{\tau}} \circ \alpha)(\mathbf{g}) = \beta_{\mathcal{K}^{\tau}}(\mathbf{g})\} \quad (62)$$

This term can be steadily combined with the one appearing in [Theorem 3.5](#) to yield a reduction of possible maps $\alpha \in \text{Vert}(\mathcal{A})$ that successfully allow a function $\beta \in \mathcal{B}^*$ to predict both $(\mathbf{y}, \mathbf{y}^{\tau})$ consistently. Notice that,

in the limit where the augmented knowledge comprehends enough additional labels and the support covers the whole, the only admitted solutions consist of:

$$(\beta_{y_\tau} \circ \text{id})(\mathbf{g}) = \underbrace{(\beta_{y_\tau} \circ \phi^{-1})}_{=:\beta_{y_\tau}} \circ \underbrace{\phi}_{=:\alpha}(\mathbf{g}) \quad (63)$$

for all $\mathbf{g} \in \mathcal{G}$, where $\phi : \mathcal{G} \rightarrow \mathcal{C}$ is an invertible function. This shows that α can be only a bijection from \mathcal{G} to \mathcal{C} . Provided all the concept vectors $\mathbf{g} \in \mathcal{G}$, the number of such possible α 's amounts to the number of possible permutation of the $|\mathcal{G}|$ elements, that is $|\mathcal{G}|!$.

D.2 Concept supervision

The count reduction was studied in [Marconato et al., 2023b], and here we report the same term. Consider the case where we supply concept supervision for a subset of concepts $\mathbf{G}_{\mathcal{I}} \subseteq \mathbf{G}$, with $\mathcal{I} \subseteq [k]$, and then augmenting the log-likelihood objective with a cross-entropy loss over the concepts: $\sum_{i \in \mathcal{I}} \log p_\theta(C_i = g_i | \mathbf{x})$. We consider also a subset $\mathcal{G}^C \subseteq \text{supp}(p^*(\mathbf{G}))$ where this supervision is provided. The constraint on the number of deterministic α 's is given by the following

$$\mathbb{I}\{\bigwedge_{\mathbf{g} \in \mathcal{G}^C} \bigwedge_{i \in \mathcal{I}} \alpha_i(\mathbf{g}) = g_i\} \quad (64)$$

If $\mathcal{I} = [k]$ and $\mathcal{G}^C = \mathcal{G}$, then we get $\alpha \equiv \text{id}$. Naturally, this requires dense annotations for all possible inputs, which may be prohibitive.

D.3 Knowledge distillation

We consider the case where samples $(\mathbf{g}, \beta^*(\mathbf{g}))$ are used to distill the ground-truth knowledge. Since by Assumption 3.2 the ground-truth inference layer is deterministic, we consider the following objective for distillation. Given a subset $\mathcal{G}^K \subseteq \text{supp}(p^*(\mathbf{G}))$ the original log-likelihood objective is complemented with the following cross-entropy:

$$\sum_{\mathbf{g} \in \mathcal{G}^K} \log \omega(\mathbb{I}\{\mathbf{C} = \mathbf{g}\})_{\beta^*(\mathbf{g})} \quad (65)$$

i.e., the $\beta^*(\mathbf{g})$ component of the CBM ω is increased for each $\mathbf{g} \in \mathcal{G}^K$. Turned to a constraint on β this can be written as follows:

$$\mathbb{I}\{\bigwedge_{\mathbf{g} \in \mathcal{G}^K} \beta(\mathbf{g}) = \beta^*(\mathbf{g})\} \quad (66)$$

When $\mathcal{G}^K = \mathcal{G}$ it necessarily holds that $\beta \equiv \beta^*$.

D.4 Reconstruction penalty

When focusing on reconstructing the input from the bottleneck, the probability distributions $p(\mathbf{C} | \mathbf{X})$ may not carry enough information to completely determine the input. In fact, if \mathbf{X} depends also on stylistic variables $\mathbf{S} \in \mathbb{R}^q$, it becomes impossible solely from \mathbf{G} to determine the input. This means that training a decoder only passing $\mathbf{c} \sim p(\mathbf{C} | \mathbf{X})$ would not convey enough information and would reduce the benefits of the reconstruction term. Marconato et al. [2023b] have studied this setting and proposed to also include additional variables $\mathbf{Z} \in \mathbb{R}^q$ in the bottleneck to overcome this problem. The encoder/decoder architecture works as follows: first the input \mathbf{x} is encoded into $p(\mathbf{C}, \mathbf{Z} | \mathbf{x})$ by the model and after sampling $(\mathbf{c}, \mathbf{z}) \sim p(\mathbf{C}, \mathbf{Z} | \mathbf{x})$ the decoder \mathbf{d} reconstruct the an input image $\hat{\mathbf{x}} = \mathbf{d}(\mathbf{c}, \mathbf{z})$. Following, under the assumption of *content-style separation*, i.e., both the encoder and the decoder process independently the concept and the stylistic variables, it holds that the constraint fr maps $\alpha \in \text{Vert}(\mathcal{A})$ given by the reconstruction penalty result in:

$$\mathbb{I}\{\bigwedge_{\mathbf{g}, \mathbf{g}' \in \text{supp}(\mathbf{G}): \mathbf{g} \neq \mathbf{g}'} \alpha(\mathbf{g}) \neq \alpha(\mathbf{g}')\} \quad (67)$$

The proof for this can be found in [Marconato et al., 2023b, Proposition 6]. Notice that, with full support over \mathcal{G} , the only such maps α must not confuse one concept vector for another, i.e., at most there are at most $|\mathcal{G}|!$ different valid α 's that are essentially a bijection from \mathcal{G} to \mathcal{C} .

E Models that satisfy Assumption 3.7

E.1 Theoretical analysis

Deep Symbolic Learning [Daniele et al., 2023]. At inference time, this method predicts a concept vector $\mathbf{c} \in \mathcal{C}$ from a conditional probability concept distributions, that is it implements a function $\mathbf{f}_{DSL} : \mathbb{R}^n \rightarrow \mathcal{C}$

where:

$$\mathbf{f}_{DSL}(\mathbf{x}) := \operatorname{argmax}_{\mathbf{c} \in \mathcal{C}} \tilde{p}(\mathbf{c} | \mathbf{x}) \quad (68)$$

where $p(\mathbf{C} | \mathbf{X})$ is a learned conditional distribution on concepts.⁶ From this expression, $\alpha \in \mathcal{A}$ is defined as:

$$\alpha(\mathbf{g}) := \mathbb{E}_{\mathbf{x} \sim p^*(\mathbf{X} | \mathbf{g})} [\mathbb{1}\{\mathbf{C} = \mathbf{f}_{DSL}(\mathbf{x})\}] \quad (69)$$

Notice that, the learned $\beta : \mathcal{G} \rightarrow \Delta_{\mathcal{Y}}$ consists in a look up table from concepts vectors $\mathbf{c} \in \mathcal{C}$, thereby the giving the conditional distribution:

$$p_{DSL}(\mathbf{Y} | \mathbf{g}) := \mathbb{E}_{\mathbf{x} \sim p^*(\mathbf{X} | \mathbf{g})} [\beta(\mathbf{f}_{DSL}(\mathbf{x}))] \quad (70)$$

By considering the measure defined by $p^*(\mathbf{x} | \mathbf{g})d\mathbf{x}$ and the transformation $\mathbf{c} = \mathbf{f}_{DSL}(\mathbf{x})$, we can pass to the new measure $p(\mathbf{c} | \mathbf{g}) = \alpha(\mathbf{g})$ obtaining:

$$p_{DSL}(\mathbf{Y} | \mathbf{g}) = \sum_{\mathbf{c} \in \mathcal{C}} \beta(\mathbf{c})p(\mathbf{c} | \mathbf{g}) \quad (71)$$

$$= \sum_{\mathbf{c} \in \mathcal{C}} \beta(\mathbf{c})\alpha(\mathbf{g})_{\mathbf{c}} \quad (72)$$

$$= (\omega_{DSL} \circ \alpha)(\mathbf{g}) \quad (73)$$

with ω that is defined as:

$$\omega_{DSL}(p(\mathbf{C})) := \sum_{\mathbf{c} \in \mathcal{C}} \beta(\mathbf{c})p(\mathbf{C} = \mathbf{c}) \quad (74)$$

This form is the same of probabilistic logic methods and we discuss the validity of [Assumption 3.7](#) along with them.

Probabilistic Logic Models. For models like DPL [[Manhaeve et al., 2018](#)], SL [[Xu et al., 2018](#)], and SPL [[Ahmed et al., 2022](#)], ω is defined as follows:

$$\omega(p(\mathbf{C})) := \sum_{\mathbf{c} \in \mathcal{C}} \beta(\mathbf{c})p(\mathbf{C} = \mathbf{c}) \quad (75)$$

Consider $\mathbf{c}, \mathbf{c}' \in \mathcal{C}$ such that:

$$\beta(\mathbf{c}) \neq \beta(\mathbf{c}') \quad (76)$$

Then, for any choice of $\lambda \in (0, 1)$ it holds:

$$\omega(\lambda \mathbb{1}\{\mathbf{C} = \mathbf{c}\} + (1 - \lambda) \mathbb{1}\{\mathbf{C} = \mathbf{c}'\}) = \lambda \beta(\mathbf{c}) + (1 - \lambda) \beta(\mathbf{c}') \quad (77)$$

$$\implies \max_{\mathbf{y} \in \mathcal{Y}} \omega(\lambda \mathbb{1}\{\mathbf{C} = \mathbf{c}\} + (1 - \lambda) \mathbb{1}\{\mathbf{C} = \mathbf{c}'\})_{\mathbf{y}} = \max_{\mathbf{y} \in \mathcal{Y}} (\lambda \beta(\mathbf{c})_{\mathbf{y}} + (1 - \lambda) \beta(\mathbf{c}')_{\mathbf{y}}) \quad (78)$$

Notice that for all $\mathbf{y} \in \mathcal{Y}$, it holds that by the convexity of the max operator:

$$\max_{\mathbf{y} \in \mathcal{Y}} (\lambda \beta(\mathbf{c})_{\mathbf{y}} + (1 - \lambda) \beta(\mathbf{c}')_{\mathbf{y}}) \leq \lambda \max_{\mathbf{y} \in \mathcal{Y}} \beta(\mathbf{c})_{\mathbf{y}} + (1 - \lambda) \max_{\mathbf{y} \in \mathcal{Y}} \beta(\mathbf{c}')_{\mathbf{y}} \quad (79)$$

$$= \max_{\mathbf{y} \in \mathcal{Y}} (\beta(\mathbf{c})_{\mathbf{y}}, \beta(\mathbf{c}')_{\mathbf{y}}) \quad (80)$$

where the equality holds if and only if $\operatorname{argmax}_{\mathbf{y} \in \mathcal{Y}} \beta(\mathbf{c})_{\mathbf{y}} = \operatorname{argmax}_{\mathbf{y} \in \mathcal{Y}} \beta(\mathbf{c}')_{\mathbf{y}}$ and $\max_{\mathbf{y} \in \mathcal{Y}} \beta(\mathbf{c})_{\mathbf{y}} = \max_{\mathbf{y} \in \mathcal{Y}} \beta(\mathbf{c}')_{\mathbf{y}}$. This proves that probabilistic logic methods satisfy [Assumption 3.7](#).

Concept Bottleneck Models. We consider CBNMs implementing a linear layer as $\omega : \Delta_{\mathcal{C}} \rightarrow \Delta_{\mathcal{Y}}$, as customary [[Koh et al., 2020](#)]. We consider the general case where the linear layer consists of a matrix $\mathbf{W} \in \mathbb{R}^{a \times b}$ with $a := |\mathcal{G}|$ rows and $b := |\mathcal{Y}|$ columns. In this setting, a probability distribution $p(\mathbf{C}) \in \Delta_{\mathcal{C}}$ corresponds to the input vector that is passed to the inference layer ω , implemented by the linear layer \mathbf{W} and a softmax operator. We denote with $w_c^y := \mathbf{W}_{c,y}$, corresponding to the (c, y) component of the matrix. The index c (resp. y) also correspond to the concept vector $\mathbf{c} \in \mathcal{C}$ (resp. \mathbf{y}), associated to it, e.g., $\mathbf{c} = (0, 1)^\top \in \{0, 1\}^2$ corresponds to $c = 1$. Following, we just use \mathbf{c} and \mathbf{y} to denote their corresponding index of the concepts and of the labels.

⁶In this case, we have that $\mathbf{f}_{DSL}(\mathbf{X}) \neq \tilde{p}(\mathbf{C} | \mathbf{X})$.

Provided a concept probability vector $\mathbf{p} \in \Delta_{\mathcal{C}}$, with components $\mathbf{p}_{\mathbf{c}} = p(\mathbf{C} = \mathbf{c})$, the conditional distribution over labels is given by the softmax operator:

$$p(\mathbf{y} \mid \mathbf{c}) = \omega(\mathbf{p})_{\mathbf{y}} \quad (81)$$

$$= \frac{\exp\left(\sum_{\mathbf{c} \in \mathcal{C}} \mathbf{W}_{\mathbf{c}, \mathbf{y}} \mathbf{p}_{\mathbf{c}}\right)}{\sum_{\mathbf{y}' \in \mathcal{Y}} \exp\left(\sum_{\mathbf{c} \in \mathcal{C}} \mathbf{W}_{\mathbf{c}, \mathbf{y}'} \mathbf{p}_{\mathbf{c}}\right)} \quad (82)$$

$$= \frac{\exp\left(\sum_{\mathbf{c} \in \mathcal{C}} \mathbf{w}_{\mathbf{c}}^{\mathbf{y}} \mathbf{p}_{\mathbf{c}}\right)}{\sum_{\mathbf{y}' \in \mathcal{Y}} \exp\left(\sum_{\mathbf{c} \in \mathcal{C}} \mathbf{w}_{\mathbf{c}}^{\mathbf{y}'} \mathbf{p}_{\mathbf{c}}\right)} \quad (83)$$

In general, for any random choice of weights \mathbf{W} , the CBNM may not satisfy [Assumption 3.7](#). Notice also that, because of the form of ω , the CBNM cannot express deterministic $\beta \in \mathcal{B}$. We consider the particular case associated with optimal models expressing an almost deterministic conditional distribution $\beta \in \mathcal{B}$, where a subset of weights $\mathbf{w}_{\mathbf{c}}^{\mathbf{y}}$ is extremely high or low. Notice that this is relevant for models in the context of [Assumption 3.2](#), where $\beta^* \in \text{Vert}(\mathcal{B})$. We can see that in order for this to happen, we need the function β to be peaked on concept vectors $\mathbf{c} \in \mathcal{C}$. This can happen only when the magnitude of one $\mathbf{w}_{\mathbf{c}}^{\mathbf{y}}$ is much higher than other $\mathbf{w}_{\mathbf{c}}^{\mathbf{y}'}$. Hence, we formulate the following condition for CBNM:

Definition E.1. Consider a CBNM $(\mathbf{f}, \omega) \in \mathcal{F} \times \Omega$ with weights $\mathbf{W} = \{\mathbf{w}_{\mathbf{c}}^{\mathbf{y}}\}$ and $M > |\mathcal{Y}| - 1$. We say that the CBNM is $\log(M)$ -deterministic at the vertices if for all $\mathbf{c} \in \mathcal{C}$, there exists $\mathbf{y} \in \mathcal{Y}$ such that:

$$\forall \mathbf{y}' \neq \mathbf{y}, \mathbf{w}_{\mathbf{c}}^{\mathbf{y}} - \mathbf{w}_{\mathbf{c}}^{\mathbf{y}'} \geq \log M \quad (84)$$

$$\forall \mathbf{y}' \neq \mathbf{y} \neq \mathbf{y}'', |\mathbf{w}_{\mathbf{c}}^{\mathbf{y}'} - \mathbf{w}_{\mathbf{c}}^{\mathbf{y}''}| \leq \log M \quad (85)$$

To see why this is helpful, we show that this constrained version of CBNM can flexibly approximate deterministic β 's:

Proposition E.2. Consider a $\log(M)$ -deterministic CBNM $(\mathbf{f}, \omega) \in \mathcal{F} \times \Omega$. It holds:

$$\forall \mathbf{c} \in \mathcal{C}, \max_{\mathbf{y} \in \mathcal{Y}} \omega(\mathbf{c})_{\mathbf{y}} \geq \frac{1}{1 + (|\mathcal{Y}| - 1)/M} \quad (86)$$

In particular, it holds that:

$$\forall \mathbf{c} \in \mathcal{C}, \lim_{M \rightarrow +\infty} \max_{\mathbf{y}} \omega(\mathbf{c})_{\mathbf{y}} = 1 \quad (87)$$

Proof. For $\mathbf{c} \in \mathcal{C}$, let $\mathbf{y} = \arg\max_{\mathbf{y}'} \omega(\mathbb{1}\{\mathbf{C} = \mathbf{c}\})_{\mathbf{y}'}$. We consider the expression:

$$\omega(\mathbb{1}\{\mathbf{C} = \mathbf{c}\}) = \frac{\exp \mathbf{w}_{\mathbf{c}}^{\mathbf{y}}}{\sum_{\mathbf{y}' \in \mathcal{C}} \exp \mathbf{w}_{\mathbf{c}}^{\mathbf{y}'}} \quad (88)$$

$$= \frac{1}{1 + \sum_{\mathbf{y}' \neq \mathbf{y}} \exp(-\mathbf{w}_{\mathbf{c}}^{\mathbf{y}} + \mathbf{w}_{\mathbf{c}}^{\mathbf{y}'})} \quad (89)$$

We now make use of the fact that the CBNM is $\log M$ -deterministic and use [Eq. \(84\)](#) to get:

$$\frac{1}{1 + \sum_{\mathbf{y}' \neq \mathbf{y}} \exp(-\mathbf{w}_{\mathbf{c}}^{\mathbf{y}} + \mathbf{w}_{\mathbf{c}}^{\mathbf{y}'})} \geq \frac{1}{1 + \sum_{\mathbf{y}' \neq \mathbf{y}} \exp -\log M} \quad (90)$$

$$= \frac{1}{1 + \sum_{\mathbf{y}' \neq \mathbf{y}} \frac{1}{M}} \quad (91)$$

$$= \frac{1}{1 + (|\mathcal{Y}| - 1)/M} \quad (92)$$

giving overall that:

$$\max_{\mathbf{y} \in \mathcal{Y}} \omega(\mathbf{c})_{\mathbf{y}} \geq \frac{1}{1 + (|\mathcal{Y}| - 1)/M} \quad (93)$$

Now, consider the limit for large $M \in \mathbb{R}$:

$$\lim_{M \rightarrow +\infty} \max_{\mathbf{y} \in \mathcal{Y}} \omega(\mathbf{c})_{\mathbf{y}} \geq \lim_{M \rightarrow +\infty} \frac{1}{1 + (|\mathcal{Y}| - 1)/M} = 1 \quad (94)$$

This concludes the proof. \square

The last point of [Proposition E.2](#) shows a viable way to get peaked label distributions from a $\log(M)$ -deterministic CBNM. This limit guaranteed that such constrained CBNMs can get closer to achieve optimal likelihood. We are now ready to prove that a $\log(M)$ -deterministic CBNM respect [Assumption 3.7](#).

Proposition E.3. *A CBNM $(f, \omega) \in \mathcal{F} \times \Omega$ that is $\log(M)$ -deterministic ([Definition E.1](#)) satisfies [Assumption 3.7](#), i.e., for all $\lambda \in (0, 1)$ and for all $\mathbf{c} \neq \mathbf{c}'$ such that $\operatorname{argmax}_{y \in \mathcal{Y}} \omega(\mathbb{1}\{\mathbf{C} = \mathbf{c}\})_y \neq \operatorname{argmax}_{y \in \mathcal{Y}} \omega(\mathbb{1}\{\mathbf{C} = \mathbf{c}'\})_y$, it holds :*

$$\max_{y \in \mathcal{Y}} \omega(\lambda \mathbb{1}\{\mathbf{C} = \mathbf{c}_1\} + (1 - \lambda) \mathbb{1}\{\mathbf{C} = \mathbf{c}_2\})_y < \max_{y \in \mathcal{Y}} (\max_{y \in \mathcal{Y}} \omega(\mathbb{1}\{\mathbf{C} = \mathbf{c}_1\})_y, \max_{y \in \mathcal{Y}} \omega(\mathbb{1}\{\mathbf{C} = \mathbf{c}_2\})_y) \quad (95)$$

Proof. Let $\mathbf{y}_1 := \operatorname{argmax}_{y \in \mathcal{Y}} \omega(\mathbb{1}\{\mathbf{C} = \mathbf{c}_1\})_y$ and $\mathbf{y}_2 := \operatorname{argmax}_{y \in \mathcal{Y}} \omega(\mathbb{1}\{\mathbf{C} = \mathbf{c}_2\})_y$ and $\lambda_1 := \lambda$ and $\lambda_2 := 1 - \lambda$, with $\lambda \in (0, 1)$ and $\mathbf{y}_1 \neq \mathbf{y}_2$. The proof is divided in two steps.

We first check that (1) the values taken by $\omega(\lambda \mathbb{1}\{\mathbf{C} = \mathbf{c}_1\} + (1 - \lambda) \mathbb{1}\{\mathbf{C} = \mathbf{c}_2\})_{\mathbf{y}_i}$, for $i \in \{1, 2\}$, are lower than those taken at the extremes. The explicit expression for $\omega(\cdot)_{\mathbf{y}_1}$ is given by:

$$\omega(\lambda_1 \mathbb{1}\{\mathbf{C} = \mathbf{c}_1\} + \lambda_2 \mathbb{1}\{\mathbf{C} = \mathbf{c}_2\})_{\mathbf{y}_1} = \frac{e^{\lambda_1 \mathbf{w}_{\mathbf{c}_1}^{\mathbf{y}_1} + \lambda_2 \mathbf{w}_{\mathbf{c}_2}^{\mathbf{y}_1}}}{\sum_{y \in \mathcal{Y}} e^{\lambda_1 \mathbf{w}_{\mathbf{c}_1}^y + \lambda_2 \mathbf{w}_{\mathbf{c}_2}^y}} \quad (96)$$

We take the derivative over λ , using that $\partial \lambda_1 / \partial \lambda = 1$ and $\partial \lambda_2 / \partial \lambda = -1$. Let $Z(\lambda) := \sum_{y \in \mathcal{Y}} \exp(\lambda_1 \mathbf{w}_{\mathbf{c}_1}^y + \lambda_2 \mathbf{w}_{\mathbf{c}_2}^y)$. We first evaluate the derivative of this expression:

$$\frac{\partial Z(\lambda)}{\partial \lambda} = \sum_{y \in \mathcal{Y}} \frac{\partial}{\partial \lambda} e^{\lambda_1 \mathbf{w}_{\mathbf{c}_1}^y + \lambda_2 \mathbf{w}_{\mathbf{c}_2}^y} \quad (97)$$

$$= \sum_{y \in \mathcal{Y}} e^{\lambda_1 \mathbf{w}_{\mathbf{c}_1}^y + \lambda_2 \mathbf{w}_{\mathbf{c}_2}^y} (\partial_\lambda \lambda_1 \mathbf{w}_{\mathbf{c}_1}^y + \partial_\lambda \lambda_2 \mathbf{w}_{\mathbf{c}_2}^y) \quad (98)$$

$$= \sum_{y \in \mathcal{Y}} e^{\lambda_1 \mathbf{w}_{\mathbf{c}_1}^y + \lambda_2 \mathbf{w}_{\mathbf{c}_2}^y} (\mathbf{w}_{\mathbf{c}_1}^y - \mathbf{w}_{\mathbf{c}_2}^y) \quad (99)$$

$$= Z(\lambda) \sum_{y \in \mathcal{Y}} \frac{e^{\lambda_1 \mathbf{w}_{\mathbf{c}_1}^y + \lambda_2 \mathbf{w}_{\mathbf{c}_2}^y}}{Z(\lambda)} (\mathbf{w}_{\mathbf{c}_1}^y - \mathbf{w}_{\mathbf{c}_2}^y) \quad (100)$$

$$= Z(\lambda) \sum_{y \in \mathcal{Y}} (\mathbf{w}_{\mathbf{c}_1}^y - \mathbf{w}_{\mathbf{c}_2}^y) \omega(\lambda_1 \mathbb{1}\{\mathbf{C} = \mathbf{c}_1\} + \lambda_2 \mathbb{1}\{\mathbf{C} = \mathbf{c}_2\})_y \quad (101)$$

Using this result we get:

$$\frac{\partial}{\partial \lambda} \frac{e^{\lambda_1 \mathbf{w}_{\mathbf{c}_1}^{\mathbf{y}_1} + \lambda_2 \mathbf{w}_{\mathbf{c}_2}^{\mathbf{y}_1}}}{Z(\lambda)} = \frac{\partial_\lambda e^{\lambda_1 \mathbf{w}_{\mathbf{c}_1}^{\mathbf{y}_1} + \lambda_2 \mathbf{w}_{\mathbf{c}_2}^{\mathbf{y}_1}} Z(\lambda) - e^{\lambda_1 \mathbf{w}_{\mathbf{c}_1}^{\mathbf{y}_1} + \lambda_2 \mathbf{w}_{\mathbf{c}_2}^{\mathbf{y}_1}} \partial_\lambda Z(\lambda)}{Z(\lambda)^2} \quad (102)$$

$$= \frac{e^{\lambda_1 \mathbf{w}_{\mathbf{c}_1}^{\mathbf{y}_1} + \lambda_2 \mathbf{w}_{\mathbf{c}_2}^{\mathbf{y}_1}} (\mathbf{w}_{\mathbf{c}_1}^{\mathbf{y}_1} - \mathbf{w}_{\mathbf{c}_2}^{\mathbf{y}_1}) Z(\lambda) - e^{\lambda_1 \mathbf{w}_{\mathbf{c}_1}^{\mathbf{y}_1} + \lambda_2 \mathbf{w}_{\mathbf{c}_2}^{\mathbf{y}_1}} Z(\lambda) \sum_{y \in \mathcal{Y}} (\mathbf{w}_{\mathbf{c}_1}^y - \mathbf{w}_{\mathbf{c}_2}^y) \omega(\lambda_1 \mathbb{1}\{\mathbf{C} = \mathbf{c}_1\} + \lambda_2 \mathbb{1}\{\mathbf{C} = \mathbf{c}_2\})_y}{Z(\lambda)^2} \quad (103)$$

$$= \frac{e^{\lambda_1 \mathbf{w}_{\mathbf{c}_1}^{\mathbf{y}_1} + \lambda_2 \mathbf{w}_{\mathbf{c}_2}^{\mathbf{y}_1}} (\mathbf{w}_{\mathbf{c}_1}^{\mathbf{y}_1} - \mathbf{w}_{\mathbf{c}_2}^{\mathbf{y}_1}) - e^{\lambda_1 \mathbf{w}_{\mathbf{c}_1}^{\mathbf{y}_1} + \lambda_2 \mathbf{w}_{\mathbf{c}_2}^{\mathbf{y}_1}} \sum_{y \in \mathcal{Y}} (\mathbf{w}_{\mathbf{c}_1}^y - \mathbf{w}_{\mathbf{c}_2}^y) \omega(\lambda_1 \mathbb{1}\{\mathbf{C} = \mathbf{c}_1\} + \lambda_2 \mathbb{1}\{\mathbf{C} = \mathbf{c}_2\})_y}{Z(\lambda)} \quad (104)$$

$$= \frac{e^{\lambda_1 \mathbf{w}_{\mathbf{c}_1}^{\mathbf{y}_1} + \lambda_2 \mathbf{w}_{\mathbf{c}_2}^{\mathbf{y}_1}} ((\mathbf{w}_{\mathbf{c}_1}^{\mathbf{y}_1} - \mathbf{w}_{\mathbf{c}_2}^{\mathbf{y}_1}) - \sum_{y \in \mathcal{Y}} (\mathbf{w}_{\mathbf{c}_1}^y - \mathbf{w}_{\mathbf{c}_2}^y) \omega(\lambda_1 \mathbb{1}\{\mathbf{C} = \mathbf{c}_1\} + \lambda_2 \mathbb{1}\{\mathbf{C} = \mathbf{c}_2\})_y)}{Z(\lambda)} \quad (105)$$

For this expression we study the sign of the derivative. Notice that we can focus only on the following term since the others are always positive

$$(\mathbf{w}_{\mathbf{c}_1}^{\mathbf{y}_1} - \mathbf{w}_{\mathbf{c}_2}^{\mathbf{y}_1}) - \sum_{y \in \mathcal{Y}} (\mathbf{w}_{\mathbf{c}_1}^y - \mathbf{w}_{\mathbf{c}_2}^y) \omega(\lambda_1 \mathbb{1}\{\mathbf{C} = \mathbf{c}_1\} + \lambda_2 \mathbb{1}\{\mathbf{C} = \mathbf{c}_2\})_y \quad (106)$$

From this expression, we can make use of the fact that in general, for a scalar function $f(\mathbf{x})$, we have $\mathbb{E}_{\mathbf{X}}[f(\mathbf{X})] \leq \max_{\mathbf{x}} f(\mathbf{x})$ and consider the following:

$$(\mathbf{w}_{\mathbf{c}_1}^{\mathbf{y}_1} - \mathbf{w}_{\mathbf{c}_2}^{\mathbf{y}_1}) - \sum_{\mathbf{y} \in \mathcal{Y}} (\mathbf{w}_{\mathbf{c}_1}^{\mathbf{y}} - \mathbf{w}_{\mathbf{c}_2}^{\mathbf{y}}) \omega(\lambda_1 \mathbb{I}\{\mathbf{C} = \mathbf{c}_1\} + \lambda_2 \mathbb{I}\{\mathbf{C} = \mathbf{c}_2\})_{\mathbf{y}} \geq (\mathbf{w}_{\mathbf{c}_1}^{\mathbf{y}_1} - \mathbf{w}_{\mathbf{c}_2}^{\mathbf{y}_1}) - \max_{\mathbf{y} \in \mathcal{Y}} (\mathbf{w}_{\mathbf{c}_1}^{\mathbf{y}} - \mathbf{w}_{\mathbf{c}_2}^{\mathbf{y}}) \quad (107)$$

$$= (\mathbf{w}_{\mathbf{c}_1}^{\mathbf{y}_1} - \mathbf{w}_{\mathbf{c}_2}^{\mathbf{y}_1}) - (\mathbf{w}_{\mathbf{c}_1}^{\mathbf{y}_1} - \mathbf{w}_{\mathbf{c}_2}^{\mathbf{y}_1}) \quad (108)$$

$$= 0 \quad (109)$$

where in the second line we used that the maximum is given by \mathbf{y}_1 . Therefore, the derivative is always increasing in the $[0, 1]$ interval, meaning that:

$$\forall \lambda \in [0, 1], \omega(\lambda_1 \mathbb{I}\{\mathbf{C} = \mathbf{c}_1\} + \lambda_2 \mathbb{I}\{\mathbf{C} = \mathbf{c}_2\})_{\mathbf{y}_1} \leq \omega(\mathbb{I}\{\mathbf{C} = \mathbf{c}_1\})_{\mathbf{y}_1} \quad (110)$$

where the equality holds if and only if $\lambda = 1$. Similarly, the derivative for $\omega(\cdot)_{\mathbf{y}_2}$ gives:

$$\begin{aligned} & \frac{\partial \omega(\lambda_1 \mathbb{I}\{\mathbf{C} = \mathbf{c}_1\} + \lambda_2 \mathbb{I}\{\mathbf{C} = \mathbf{c}_2\})_{\mathbf{y}_2}}{\partial \lambda} \\ &= \frac{e^{\lambda_1 \mathbf{w}_{\mathbf{c}_1}^{\mathbf{y}_2} + \lambda_2 \mathbf{w}_{\mathbf{c}_2}^{\mathbf{y}_2}} ((\mathbf{w}_{\mathbf{c}_1}^{\mathbf{y}_2} - \mathbf{w}_{\mathbf{c}_2}^{\mathbf{y}_2}) - \sum_{\mathbf{y} \in \mathcal{Y}} (\mathbf{w}_{\mathbf{c}_1}^{\mathbf{y}} - \mathbf{w}_{\mathbf{c}_2}^{\mathbf{y}}) \omega(\lambda_1 \mathbb{I}\{\mathbf{C} = \mathbf{c}_1\} + \lambda_2 \mathbb{I}\{\mathbf{C} = \mathbf{c}_2\})_{\mathbf{y}})}{Z(\lambda)} \end{aligned} \quad (111)$$

By using the fact that $\mathbb{E}_{\mathbf{X}}[f(\mathbf{X})] \geq \min_{\mathbf{x}} f(\mathbf{x})$ for a scalar function $f(\mathbf{x})$, we obtain:

$$(\mathbf{w}_{\mathbf{c}_1}^{\mathbf{y}_2} - \mathbf{w}_{\mathbf{c}_2}^{\mathbf{y}_2}) - \sum_{\mathbf{y} \in \mathcal{Y}} (\mathbf{w}_{\mathbf{c}_1}^{\mathbf{y}} - \mathbf{w}_{\mathbf{c}_2}^{\mathbf{y}}) \omega(\lambda_1 \mathbb{I}\{\mathbf{C} = \mathbf{c}_1\} + \lambda_2 \mathbb{I}\{\mathbf{C} = \mathbf{c}_2\})_{\mathbf{y}} \leq (\mathbf{w}_{\mathbf{c}_1}^{\mathbf{y}_2} - \mathbf{w}_{\mathbf{c}_2}^{\mathbf{y}_2}) - \min_{\mathbf{y} \in \mathcal{Y}} (\mathbf{w}_{\mathbf{c}_1}^{\mathbf{y}} - \mathbf{w}_{\mathbf{c}_2}^{\mathbf{y}}) \quad (112)$$

$$= (\mathbf{w}_{\mathbf{c}_1}^{\mathbf{y}_2} - \mathbf{w}_{\mathbf{c}_2}^{\mathbf{y}_2}) - (\mathbf{w}_{\mathbf{c}_1}^{\mathbf{y}_2} - \mathbf{w}_{\mathbf{c}_2}^{\mathbf{y}_2}) \quad (113)$$

$$= 0 \quad (114)$$

where in the second line we used that the minimum is given by \mathbf{y}_2 . Hence, the derivative is always decreasing for $\lambda \in [0, 1]$ and it holds:

$$\forall \lambda \in [0, 1], \omega(\lambda_1 \mathbb{I}\{\mathbf{C} = \mathbf{c}_1\} + \lambda_2 \mathbb{I}\{\mathbf{C} = \mathbf{c}_2\})_{\mathbf{y}_2} \leq \omega(\mathbb{I}\{\mathbf{C} = \mathbf{c}_2\})_{\mathbf{y}_2} \quad (115)$$

where the equality holds if and only if $\lambda = 0$.

(2) Now, we check the same holds when choosing another element $\mathbf{y}' \neq \mathbf{y}_1, \mathbf{y}_2$. To this end, we consider the following expressions:

$$\frac{p(\mathbf{y} \mid \lambda_1 \mathbb{I}\{\mathbf{C} = \mathbf{c}_1\} + \lambda_2 \mathbb{I}\{\mathbf{C} = \mathbf{c}_2\})}{p(\mathbf{y}_1 \mid \mathbf{c}_1)}, \quad \frac{p(\mathbf{y} \mid \lambda_1 \mathbb{I}\{\mathbf{C} = \mathbf{c}_1\} + \lambda_2 \mathbb{I}\{\mathbf{C} = \mathbf{c}_2\})}{p(\mathbf{y}_2 \mid \mathbf{c}_2)} \quad (116)$$

where $p(\mathbf{y} \mid \mathbf{p}) := \omega(\mathbf{p})_{\mathbf{y}}$. Consider the first expression. We can rewrite it as follows:

$$\frac{p(\mathbf{y} \mid \lambda_1 \mathbb{I}\{\mathbf{C} = \mathbf{c}_1\} + \lambda_2 \mathbb{I}\{\mathbf{C} = \mathbf{c}_2\})}{p(\mathbf{y}_1 \mid \mathbf{c}_1)} = \frac{p(\mathbf{y} \mid \lambda_1 \mathbb{I}\{\mathbf{C} = \mathbf{c}_1\} + \lambda_2 \mathbb{I}\{\mathbf{C} = \mathbf{c}_2\})}{p(\mathbf{y}_1 \mid \lambda_1 \mathbb{I}\{\mathbf{C} = \mathbf{c}_1\} + \lambda_2 \mathbb{I}\{\mathbf{C} = \mathbf{c}_2\})} \frac{p(\mathbf{y}_1 \mid \lambda_1 \mathbb{I}\{\mathbf{C} = \mathbf{c}_1\} + \lambda_2 \mathbb{I}\{\mathbf{C} = \mathbf{c}_2\})}{p(\mathbf{y}_1 \mid \mathbf{c}_1)} \quad (117)$$

$$\leq \frac{p(\mathbf{y} \mid \lambda_1 \mathbb{I}\{\mathbf{C} = \mathbf{c}_1\} + \lambda_2 \mathbb{I}\{\mathbf{C} = \mathbf{c}_2\})}{p(\mathbf{y}_1 \mid \lambda_1 \mathbb{I}\{\mathbf{C} = \mathbf{c}_1\} + \lambda_2 \mathbb{I}\{\mathbf{C} = \mathbf{c}_2\})} \quad (118)$$

where in the last line we made use of the fact that the second fraction in the right-hand side of the first line is always ≤ 1 . Similarly we have that:

$$\frac{p(\mathbf{y} \mid \lambda_1 \mathbb{I}\{\mathbf{C} = \mathbf{c}_1\} + \lambda_2 \mathbb{I}\{\mathbf{C} = \mathbf{c}_2\})}{p(\mathbf{y}_2 \mid \mathbf{c}_2)} \leq \frac{p(\mathbf{y} \mid \lambda_1 \mathbb{I}\{\mathbf{C} = \mathbf{c}_1\} + \lambda_2 \mathbb{I}\{\mathbf{C} = \mathbf{c}_2\})}{p(\mathbf{y}_2 \mid \lambda_1 \mathbb{I}\{\mathbf{C} = \mathbf{c}_1\} + \lambda_2 \mathbb{I}\{\mathbf{C} = \mathbf{c}_2\})} \quad (119)$$

We proceed to substituting explicitly the expression for $p(\mathbf{y} \mid \lambda_1 \mathbb{I}\{\mathbf{C} = \mathbf{c}_1\} + \lambda_2 \mathbb{I}\{\mathbf{C} = \mathbf{c}_2\})$ into the upper bound of Eq. (118):

$$\frac{p(\mathbf{y} \mid \lambda_1 \mathbb{I}\{\mathbf{C} = \mathbf{c}_1\} + \lambda_2 \mathbb{I}\{\mathbf{C} = \mathbf{c}_2\})}{p(\mathbf{y}_1 \mid \lambda_1 \mathbb{I}\{\mathbf{C} = \mathbf{c}_1\} + \lambda_2 \mathbb{I}\{\mathbf{C} = \mathbf{c}_2\})} = \frac{e^{\lambda_1 \mathbf{w}_{\mathbf{c}_1}^{\mathbf{y}} + \lambda_2 \mathbf{w}_{\mathbf{c}_2}^{\mathbf{y}}} Z(\lambda)}{e^{\lambda_1 \mathbf{w}_{\mathbf{c}_1}^{\mathbf{y}_1} + \lambda_2 \mathbf{w}_{\mathbf{c}_2}^{\mathbf{y}_1}} Z(\lambda)} \quad (120)$$

$$= \exp(\lambda_1(\mathbf{w}_{\mathbf{c}_1}^{\mathbf{y}} - \mathbf{w}_{\mathbf{c}_1}^{\mathbf{y}_1}) + \lambda_2(\mathbf{w}_{\mathbf{c}_2}^{\mathbf{y}} - \mathbf{w}_{\mathbf{c}_2}^{\mathbf{y}_1})) \quad (121)$$

$$\leq \exp(-\lambda_1 \log(M) + \lambda_2(\mathbf{w}_{\mathbf{c}_2}^{\mathbf{y}} - \mathbf{w}_{\mathbf{c}_2}^{\mathbf{y}_1}))$$

(Substituting the bound from Eq. (84))

$$\leq \exp(-\lambda_1 \log(M) + \lambda_2 \log(M))$$

(Substituting the bound from Eq. (85))

$$= M^{\lambda_2 - \lambda_1} \quad (122)$$

With similar steps and substitutions we get that:

$$\frac{p(\mathbf{y} \mid \lambda_1 \mathbb{I}\{\mathbf{C} = \mathbf{c}_1\} + \lambda_2 \mathbb{I}\{\mathbf{C} = \mathbf{c}_2\})}{p(\mathbf{y}_2 \mid \lambda_1 \mathbb{I}\{\mathbf{C} = \mathbf{c}_1\} + \lambda_2 \mathbb{I}\{\mathbf{C} = \mathbf{c}_2\})} \leq M^{\lambda_1 - \lambda_2} \quad (123)$$

Taking the product of Eq. (122) and Eq. (123) we obtain:

$$\frac{p(\mathbf{y} \mid \lambda_1 \mathbb{I}\{\mathbf{C} = \mathbf{c}_1\} + \lambda_2 \mathbb{I}\{\mathbf{C} = \mathbf{c}_2\})}{p(\mathbf{y}_1 \mid \lambda_1 \mathbb{I}\{\mathbf{C} = \mathbf{c}_1\} + \lambda_2 \mathbb{I}\{\mathbf{C} = \mathbf{c}_2\})} \cdot \frac{p(\mathbf{y} \mid \lambda_1 \mathbb{I}\{\mathbf{C} = \mathbf{c}_1\} + \lambda_2 \mathbb{I}\{\mathbf{C} = \mathbf{c}_2\})}{p(\mathbf{y}_2 \mid \lambda_1 \mathbb{I}\{\mathbf{C} = \mathbf{c}_1\} + \lambda_2 \mathbb{I}\{\mathbf{C} = \mathbf{c}_2\})}$$

$$\leq M^{\lambda_2 - \lambda_1} M^{\lambda_1 - \lambda_2} \quad (124)$$

$$= 1 \quad (125)$$

Notice also that:

$$\frac{p(\mathbf{y} \mid \lambda_1 \mathbb{I}\{\mathbf{C} = \mathbf{c}_1\} + \lambda_2 \mathbb{I}\{\mathbf{C} = \mathbf{c}_2\})}{p(\mathbf{y}_1 \mid \lambda_1 \mathbb{I}\{\mathbf{C} = \mathbf{c}_1\} + \lambda_2 \mathbb{I}\{\mathbf{C} = \mathbf{c}_2\})} \cdot \frac{p(\mathbf{y} \mid \lambda_1 \mathbb{I}\{\mathbf{C} = \mathbf{c}_1\} + \lambda_2 \mathbb{I}\{\mathbf{C} = \mathbf{c}_2\})}{p(\mathbf{y}_2 \mid \lambda_1 \mathbb{I}\{\mathbf{C} = \mathbf{c}_1\} + \lambda_2 \mathbb{I}\{\mathbf{C} = \mathbf{c}_2\})}$$

$$\geq \min \left(\frac{p(\mathbf{y} \mid \lambda_1 \mathbb{I}\{\mathbf{C} = \mathbf{c}_1\} + \lambda_2 \mathbb{I}\{\mathbf{C} = \mathbf{c}_2\})^2}{p(\mathbf{y}_1 \mid \lambda_1 \mathbb{I}\{\mathbf{C} = \mathbf{c}_1\} + \lambda_2 \mathbb{I}\{\mathbf{C} = \mathbf{c}_2\})^2}, \frac{p(\mathbf{y} \mid \lambda_1 \mathbb{I}\{\mathbf{C} = \mathbf{c}_1\} + \lambda_2 \mathbb{I}\{\mathbf{C} = \mathbf{c}_2\})^2}{p(\mathbf{y}_2 \mid \lambda_1 \mathbb{I}\{\mathbf{C} = \mathbf{c}_1\} + \lambda_2 \mathbb{I}\{\mathbf{C} = \mathbf{c}_2\})^2} \right) \quad (126)$$

which in turn means that:

$$\min \left(\frac{p(\mathbf{y} \mid \lambda_1 \mathbb{I}\{\mathbf{C} = \mathbf{c}_1\} + \lambda_2 \mathbb{I}\{\mathbf{C} = \mathbf{c}_2\})^2}{p(\mathbf{y}_1 \mid \lambda_1 \mathbb{I}\{\mathbf{C} = \mathbf{c}_1\} + \lambda_2 \mathbb{I}\{\mathbf{C} = \mathbf{c}_2\})^2}, \frac{p(\mathbf{y} \mid \lambda_1 \mathbb{I}\{\mathbf{C} = \mathbf{c}_1\} + \lambda_2 \mathbb{I}\{\mathbf{C} = \mathbf{c}_2\})^2}{p(\mathbf{y}_2 \mid \lambda_1 \mathbb{I}\{\mathbf{C} = \mathbf{c}_1\} + \lambda_2 \mathbb{I}\{\mathbf{C} = \mathbf{c}_2\})^2} \right) \leq 1 \quad (127)$$

$$\implies \min \left(\frac{p(\mathbf{y} \mid \lambda_1 \mathbb{I}\{\mathbf{C} = \mathbf{c}_1\} + \lambda_2 \mathbb{I}\{\mathbf{C} = \mathbf{c}_2\})}{p(\mathbf{y}_1 \mid \lambda_1 \mathbb{I}\{\mathbf{C} = \mathbf{c}_1\} + \lambda_2 \mathbb{I}\{\mathbf{C} = \mathbf{c}_2\})}, \frac{p(\mathbf{y} \mid \lambda_1 \mathbb{I}\{\mathbf{C} = \mathbf{c}_1\} + \lambda_2 \mathbb{I}\{\mathbf{C} = \mathbf{c}_2\})}{p(\mathbf{y}_2 \mid \lambda_1 \mathbb{I}\{\mathbf{C} = \mathbf{c}_1\} + \lambda_2 \mathbb{I}\{\mathbf{C} = \mathbf{c}_2\})} \right) \leq 1 \quad (128)$$

This last expression is in line with the condition of [Assumption 3.7](#), showing that, for all $\mathbf{y} \in \mathcal{Y}$, either $\omega(\mathbb{I}\{\mathbf{C} = \mathbf{c}_1\})_{\mathbf{y}_1}$ or $\omega(\mathbb{I}\{\mathbf{C} = \mathbf{c}_2\})_{\mathbf{y}_2}$ are greater or equal to $\omega(\lambda \mathbb{I}\{\mathbf{C} = \mathbf{c}_1\} + (1 - \lambda) \mathbb{I}\{\mathbf{C} = \mathbf{c}_2\})_{\mathbf{y}}$. Combining step (1) and (2), we obtain that [Assumption 3.7](#) holds and that:

$$\max_{\mathbf{y} \in \mathcal{Y}} \omega(\lambda \mathbb{I}\{\mathbf{C} = \mathbf{c}_1\} + (1 - \lambda) \mathbb{I}\{\mathbf{C} = \mathbf{c}_2\})_{\mathbf{y}} \leq \max \left(\max_{\mathbf{y} \in \mathcal{Y}} \omega(\mathbb{I}\{\mathbf{C} = \mathbf{c}_1\})_{\mathbf{y}}, \max_{\mathbf{y} \in \mathcal{Y}} \omega(\mathbb{I}\{\mathbf{C} = \mathbf{c}_2\})_{\mathbf{y}} \right) \quad (129)$$

where equality holds if and only if $\lambda \in \{0, 1\}$. \square

E.2 Numerical evaluation of Assumption 3.7

We investigate experimentally whether the models used in our evaluation satisfy [Assumption 3.7](#). We proved in [Appendix E.1](#) that the DSL inference layer reduces to Probabilistic Logic methods and only consider DPL and DPL* as representatives. For CBNM we conduct a separate investigation.

We first consider the case where the prior knowledge K is used to define the inference layer as customary in DPL. Accordingly, we found that [Assumption 3.7](#) is satisfied for all possible couples $(\mathbf{c}_1, \mathbf{c}_2) \in [100]^2$ that predicts distinct labels, see [Fig. 10](#).

We now turn to DPL*. Due to the linearity of the inference layer of DPL* it suffices to consider random weights as a representative for a candidate learned inference layer. Consistently, we found that for all possible couples $(\mathbf{c}_1, \mathbf{c}_2) \in [100]^2$ that predicts distinct labels, [Assumption 3.7](#) is satisfied. See [Fig. 11](#).

Finally, we evaluate explicitly whether a trained CBMM on MNIST-Add close to optimal likelihood respects, or at least is close to satisfy, [Assumption 3.7](#). We train a CBMM with 150 epochs of training, reaching a mean negative log-likelihood of 0.0884 on the test set. Notice that, due to the softmax operator, there are no choices giving zero negative log-likelihood. We found that [Assumption 3.7](#) is satisfied for the 95% of possible couples $(\mathbf{c}_1, \mathbf{c}_2) \in [100]^2$ giving different labels. For the remaining 5% the assumption is marginally violated with a maximum increase of:

$$\max_{\mathbf{c}_1, \mathbf{c}_2, \lambda} \left(\max_{\mathbf{y}} \omega(\lambda \mathbb{1}\{\mathbf{C} = \mathbf{c}_i\} + (1 - \lambda) \mathbb{1}\{\mathbf{C} = \mathbf{c}_j\})_{\mathbf{y}} - \max \left(\max_{\mathbf{y}} \omega(\mathbb{1}\{\mathbf{c}_1\})_{\mathbf{y}}, \max_{\mathbf{y}} \omega(\mathbb{1}\{\mathbf{c}_2\})_{\mathbf{y}} \right) \right) \leq 1.38 \cdot 10^{-3} \quad (130)$$

Our results on this investigation are displayed in [Fig. 12](#).

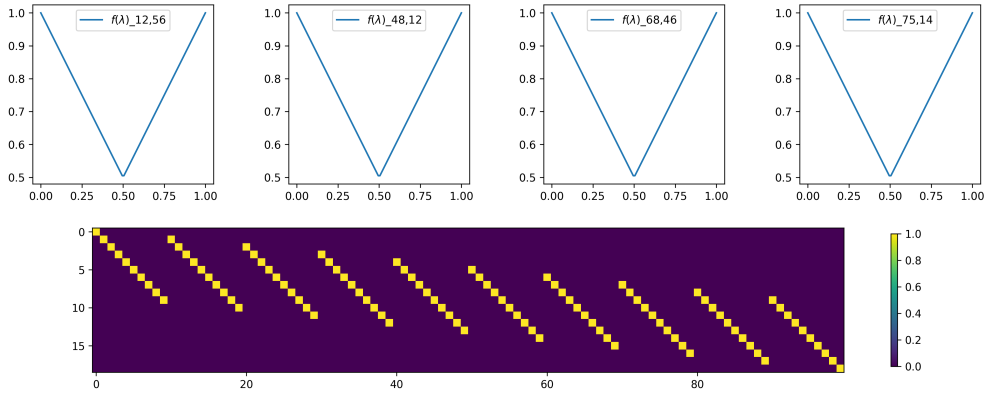


Figure 10: **The logic inference layer of DPL in MNIST-Add.** (Top) The behavior of $f(\lambda) := \max_{\mathbf{y}} \omega(\lambda \mathbb{1}\{\mathbf{C} = \mathbf{c}_i\} + (1 - \lambda) \mathbb{1}\{\mathbf{C} = \mathbf{c}_j\})$, for four pairs i, j sampled randomly from the 100 possible worlds. (Bottom) The linear layer weights for DPL.

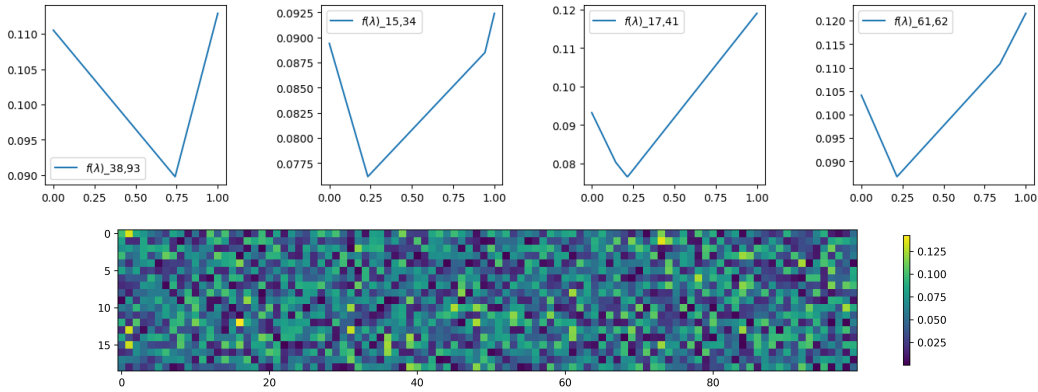


Figure 11: **A random inference layer for DPL* in MNIST-Add.** (Top) The behavior of $f(\lambda) := \max_{\mathbf{y}} \omega(\lambda \mathbb{1}\{\mathbf{C} = \mathbf{c}_i\} + (1 - \lambda) \mathbb{1}\{\mathbf{C} = \mathbf{c}_j\})$, for four pairs i, j sampled randomly from the 100 possible worlds. (Bottom) The linear layer weights for DPL*.

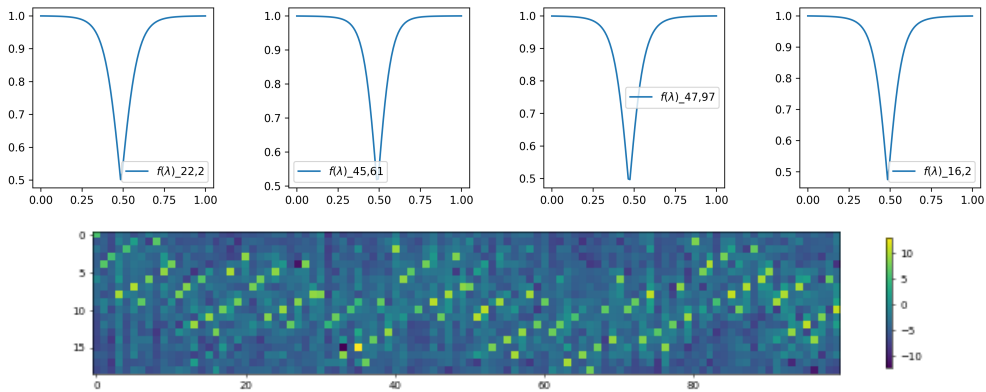


Figure 12: **Optimal CBNM in MNIST-Add.** We visualize the learned weights by a CBNM achieving maximum log-likelihood in MNIST-Add. (Top) The behavior of $f(\lambda) := \max_{\mathbf{y}} \omega(\lambda \mathbb{1}\{\mathbf{C} = \mathbf{c}_i\} + (1 - \lambda) \mathbb{1}\{\mathbf{C} = \mathbf{c}_j\})$, for four pairs i, j sampled randomly from the 100 possible worlds. The sampled pairs align with [Assumption 3.7](#). (Bottom) The linear layer weights for the trained CBNM.